The impact of rural nature-based solutions in upstream catchments on downstream flood peak magnitude and timing

Using modified soil parameters in plot-scale and catchment-scale models for the Geul catchment

by

Josien Groot

to obtain the degree of Master of Science
at the Delft University of Technology,
to be defended publicly in October, 2025

Student number: 4450728
Project duration: May, 2025 – October, 2025
Thesis committee:

dr. ir. J.A.E. ten Veldhuis,	TU Delft, Main supervisor
dr. ir. A.M.J. Coenders,	TU Delft, supervisor
dr. M. Hrachowitz,	TU Delft, supervisor

TU Delft

Preface

Writing this thesis has truly been a journey. When I started, recovering from a concussion and eventually started working a 40-hour week, it seemed almost impossible to find the focus and energy to dive deep into theory, modelling, QGIS, Python programming, and thus the long hours of staring at my computer screen. However, despite these challenges, I am extremely proud that a finished report is available and that I can hopefully call myself an engineer.

Even with a slight delay — much like the modelled flood peaks of the Geul — this process taught me stamina. It showed me that every big project becomes possible when you take it stapje voor stapje (step by step). For this, I am grateful to my main supervisor, Marie-Claire, whose practical guidance and encouragement helped me keep moving forward, one step at a time.

Along the way, I also discovered that I can truly call myself a coding geek. This skill will hopefully come in handy in the future. Thanks to my rediscovered skills, I feel more like a complete water resources engineer. I owe much of my rediscovered hydrology and water systems knowledge to the insightful meetings with the entire committee. Their expertise and feedback challenged me to look beyond the outputs and to think more deeply about the physical processes underlying the models.

"What I love most about rivers is
You can't step in the same river twice
The water's always changing
always flowing."

— Pocahontas (1995)

This resonates with me: I am no longer the person I was when I started this master's program. I have changed - personally and professionally - and I hope to carry that growth forward.

Finally, I want to thank my family, friends and, of course, my music playlists for keeping me sane throughout this journey, especially when I tended to overthink. Their support and understanding made it possible to reach this point.

Josien Groot
Delft, October 10, 2025

Abstract

Heavy rain events and flash floods, such as those in July 2021 in the Geul catchment, are projected to increase in both severity and frequency. In addition to traditional grey measures (e.g., dikes and reservoirs), rural nature-based solutions (NbS) that enhance the sponge function of the soil are being considered. However, the effectiveness of rural NbS during extreme events remains contested.

This study simulates the potential of rural nature-based solutions for flood mitigation under extreme rainfall, with a focus on river peak flows in the Geul during the July 2021 event. To this end, the combination of a physics-based plot-scale model (SWAP) and a conceptual distributed catchment model (wflow$_{sbm}$) is used. The work proceeds by: (i) comparing soil–water process representations in both models ; (ii) performing sensitivity analyses of soil parameters; (iii) designing a rural NbS scenario by modifying soil-hydraulic parameters; and (iv) evaluating the effects of these scenarios on flood hydrographs at the catchment outlet.

SWAP results show that simulated infiltration and overland flow are most sensitive to saturated water content (θ_{sat}) and saturated hydraulic conductivity (K$_{sat}$). A two meter sandy soil column would have accommodated the entire July 2021 rainfall, resulting in negligible overland flow. In wflow$_{sbm}$, sensitivity analysis indicated that simulated flood hydrographs are most influenced by KsatVer, θ_r, and θ_s. Adjusting θ_r and θ_s in downstream subcatchments could significantly improve the model's ability to match the observed hydrographs.

Scenario simulations in wflow$_{sbm}$ reveal spatially dependent effects. Downstream interventions have a damping effect on peak flow magnitude, whereas interventions in the upstream part of the Netherlands can increase it. A catchment-wide rural NbS scenario reduces the downstream peak by approximately 50% and delays the peak by approximately two hours relative to the default model. This modelled delay lies within the observed five-hour offset between the Geul and Meuse peaks in July 2021, suggesting such measures are unlikely to increase flood risk at the confluence via peak synchronization.

Keywords: Flood mitigation ; July 2021 flood ; Geul catchment ; sponge landscape ; water storage capacity, hydraulic conductivity ; SWAP ; wflow$_{sbm}$; infiltration ; overland flow ; river peak flow ; vertical unsaturated flow ; nature-based solutions ; rural hydrology

Contents

1 Introduction

1.1. Research motivation

During July 2021, several European countries, including the Netherlands, experienced severe flooding. The Geul catchment in South Limburg was the most affected region in the Netherlands, where extreme rainfall led to record discharges and widespread damage. The Intergovernmental Panel on Climate Change (IPCC) warns that such extreme weather events are likely to become more frequent and intense in the coming decades ((IPCC), 2023). This highlights the urgency of developing innovative solutions that improve water storage in the catchment and attenuate river peak flows in this catchment.

In the Geul catchment, a large portion of precipitation did not contribute to rapid runoff towards the river network. A model study by Deltares found that during the 2021 event, only about 45 mm of the 145 mm of precipitation became river discharge (Deltares, 2023). This indicates that the soil acted as a substantial buffer, highlighting the potential of using the soil and its soil-water processes to attenuate river peak flows and complement traditional grey infrastructure measures for flood mitigation in this area.

The Geul catchment is not unique in this regard. Globally, there is increasing attention toward alternative and complementary approaches to mitigate hydrologic extremes, commonly referred to as nature-based solutions (NbS) (Kumar et al., 2021). While traditional grey infrastructure measures are typically designed with the sole objective of flood protection, NbS represent an integrated approach that delivers more benefits. The European Commission defined NbS as measures that are cost-effective, inspired and supported by nature, and aimed at addressing environmental, social and economic challenges while simultaneously providing services such as carbon storage, improved water quality, improved groundwater recharge and increased biodiversity, thereby contributing to long-term resilience (European Commission, 2014; European Commission, 2015).

In the domain of river hydraulics, NbS include river remeandering and floodplain restoration (Gourevitch et al., 2020). Such measures improve floodplain storage capacity and promote natural regulation of flow dynamics, thereby reducing flow velocity and attenuating peak discharges during heavy rainfall events (Kumar et al., 2021; Baptist et al., 2004; Ruangpan et al., 2020; Penning et al., 2023).

In the field of (geo)hydrology, NbS include measures such as wetland preservation and land use changes including afforestation, agroforestry, and hedgerows. These interventions create so-called “sponge landscapes,” enhance soil infiltration capacity (Wang et al., 2015), increase water retention, and slow runoff generation. As a result, they can contribute to attenuating river peak flows and mitigating downstream flood impacts (Penning et al., 2023; Calder et al., 2003). Because these measures are implemented predominantly in rural areas, this study adopts the term *rural nature-based solutions*. Given that South Limburg is not that urbanized and largely agricultural (de Moor et al., 2008), the region provides a relevant setting to evaluate the effectiveness of such measures for (complementary) flood mitigation.

1.2. Problem statement and knowledge gap

Despite growing interest in rural NbS for flood mitigation, their quantitative effectiveness on the catchment scale remains highly uncertain. Rogger et al., 2017 highlighted the need for more process-based and quantitative assessments at this scale, as existing studies on rural NbS and runoff generation often reach contradictory conclusions (Calder et al., 2007; Bernsteinová et al., 2015; Alila et al., 2009 ; Andréassian, 2004). This uncertainty makes it difficult to assess the actual potential of rural NbS to reduce flood risk, especially under extreme rainfall conditions.

Assessing the quantitative effectiveness of rural nature-based solutions requires modelling approaches that operate at the relevant model complexity and spatial scale. This study uses the conceptual wflow Simple Bucket Model (wflow$_{sbm}$), which has already been calibrated for the Geul catchment (Klein, 2022). This enables the focus on testing scenarios rather than setting up and calibrating the model from scratch. However, a reliable simulation of flood hydrographs depends on an accurate representation of soil hydraulic properties. Plot-scale models such as SWAP (Heinen et al., 2024) provide a detailed physics-based description of these properties, with particular emphasis on unsaturated flow. Translating SWAP's parameterizations into a conceptual distributed model such as wflow$_{sbm}$ could therefore improve distributed modelling in a more physically based manner. Although both SWAP and wflow$_{sbm}$ have been widely applied in agricultural (Li and Ren, 2019) and hydrological research (Bouaziz, 2021), no studies have systematically compared their representation of soil–water processes in the context of flood mitigation.

In addition, existing studies that use distributed hydrological models to assess the impact of rural NbS mainly focus on land use-land cover changes (Overhoff and Slager, 2024). These studies typically involve modifying model parameters that reduce the proportion of compacted surfaces, increase infiltration at the soil surface, and increase surface roughness (Kwadijk et al., 2022 ; Deltares, 2023). However, they rarely consider how these changes in land use affect the hydraulic properties within the soil column itself (Overhoff and Slager, 2024). This aspect is crucial, as rural NbS are expected to enhance soil permeability (Brown et al., 2005 ; Andréassian, 2004; Alaoui et al., 2011), and overall water storage capacity (Alila et al., 2009). Addressing these gaps is essential for applying wflow$_{sbm}$ reliably as a tool to evaluate the flood mitigation potential of rural NbS.

A further knowledge gap concerns the broader system-scale effects of implementing rural NbS. While the prevailing hypothesis is that rural NbS delay and reduce peak river discharges (Zeiger and Hubbart, 2018), this effect is not universally beneficial. If delayed runoff leads to the synchronization of peak flows at the downstream confluence point, it can amplify the flood peaks and counteract the intended protective function (Saghafian et al., 2008; Yang et al., 2025). Evaluating the potential coincidence of flood peaks between the upstream catchment and its receiving basin is therefore critical to determine whether rural NbS reduce or unintentionally amplify flood risk at their confluence.

1.3. Research objective

This research aims to simulate the potential of rural nature-based solutions for flood mitigation under extreme rainfall conditions, with a specific application to river peak flows in the Geul during the heavy rainfall event of July 2021.

1.4. Scope

This is an *event-based model study* and is structured around the following:

- **Comparing** the approaches and process-level differences in soil-water modelling between SWAP and wflow$_{sbm}$.
- **Identifying** the most influential soil parameters on infiltration and overland flow generation in SWAP, and the parameters to which flood hydrographs are most sensitive in wflow$_{sbm}$.

- **Designing** rural nature-based solution scenarios in wflow$_{sbm}$ by modifying soil hydraulic parameters as a proxy.
- **Quantifying** the effects of these model scenarios on river peak discharge magnitude and timing during the July 2021 heavy rainfall event.

1.5. Research questions

Based on the defined objective and scope, this research is structured around four research questions. These questions translate the aim of understanding the hydrological soil processes in the two modelling frameworks and to simulate the potential of rural nature-based solutions to attenuate river peak flows into actionable steps.

1. Which soil parameters most strongly influence the simulated infiltration and overland flow in SWAP under the July 2021 conditions?
2. To which soil parameters in wflow$_{sbm}$ are the simulated flood hydrographs most sensitive under the July 2021 conditions?
3. How can soil parameter modifications in wflow$_{sbm}$ be used as a proxy for rural nature-based solutions?
4. How do these rural nature-based solution scenarios in wflow$_{sbm}$ affect the magnitude and timing of the simulated peak flow of the Geul catchment during the July 2021 event?

2

Study Area

This chapter introduces the Geul catchment, the case study area of this research, and outlines the characteristics of the July 2021 flood event. Understanding the geological and hydrological setting of the catchment is essential for designing and interpreting the modelling results that follow. The Geul, as an upstream tributary of the transboundary Meuse River, exerts a hydrological influence on its receiving basin. Its location, land use, and complex hydrogeology make it a suitable setting to explore how rural nature-based solutions can influence flood peak magnitude and timing.

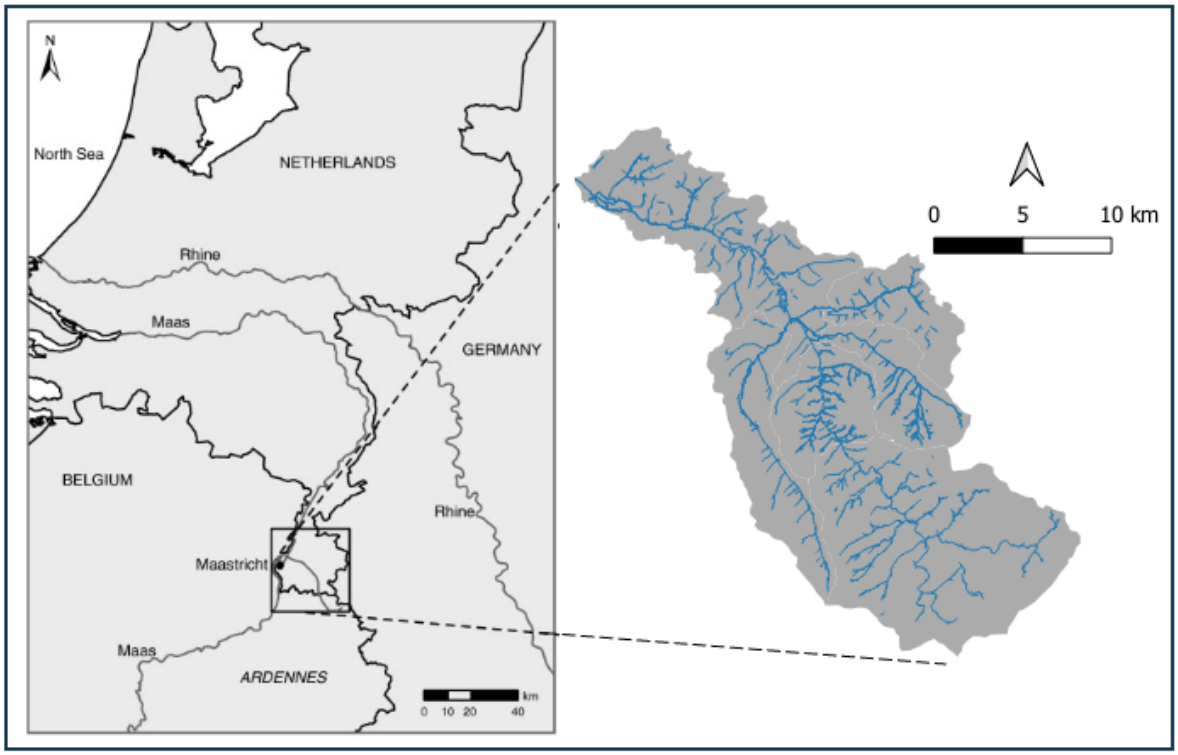

Figure 2.1: Location of the Geul catchment. (Left) Position of the Geul within the Meuse River basin in northwestern Europe. (Right) Outline of the Geul catchment with its stream network.

2.1. Meuse basin context

The Geul catchment is part of the larger Meuse basin. The Meuse river springs in France and will eventually flow into the sea in the Netherlands. The basin covers parts of France, Belgium, Germany, and the Netherlands.

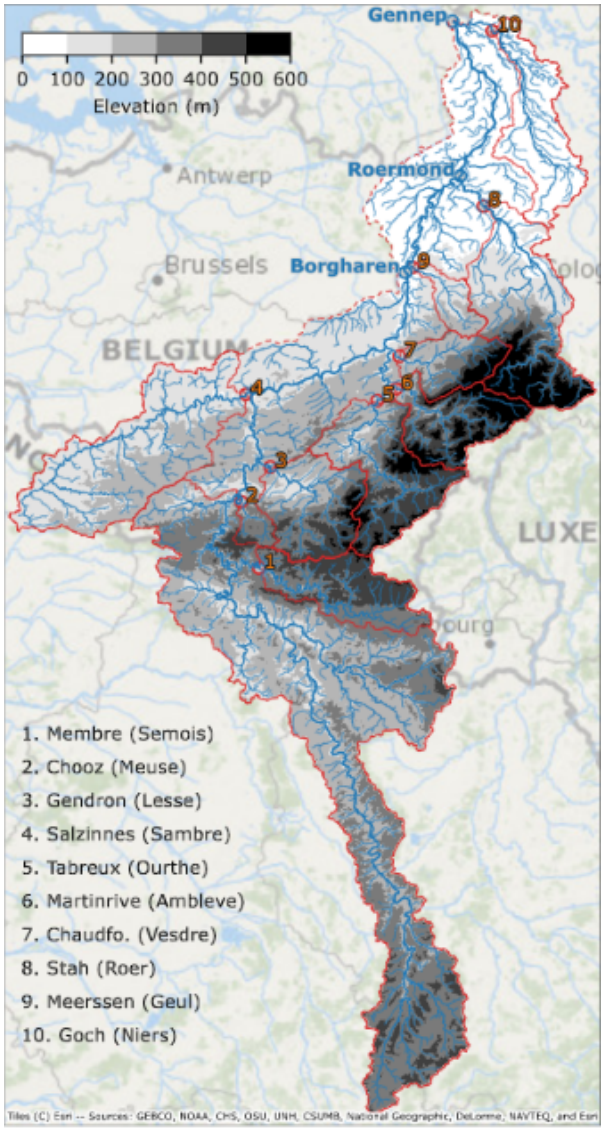

Figure 2.2: Introducing the Meuse basin with its upstream/tributary catchments (Rongen et al., 2023). The outlet of the Geul catchment is indicated at point 9 and the larger version of the figure can be found in Appendix A.

Peak discharges in the Meuse occur mainly in the winter season, when the rainfall event has a long duration, the actual evaporation is small, and snowmelt can contribute to the discharge. During these peak events, the soil is often already saturated (Ashagrie et al., 2006). The travel time for the peak discharge of the Maas is relatively short. It takes approximately 16 hours from the Belgium border (point 2 in Figure 2.2) to the Dutch border (Borgharen in Figure 2.2) (de Wit, 2008). In case of an extreme rainfall event, the Meuse peak can reach the Dutch border at Borgharen even quicker. The interesting thing is that the tributaries downstream of Chooz react faster to a rainfall event than the French tributaries (upstream of Chooz) (Rura Arnhem, 2018). Slowing down the river runoff of the downstream tributaries relative to Chooz, can therefore lead to peak synchronization and increase the total peak discharge in the main river (Saghafian et al., 2008).

2.2. Topography and climate

The Geul river is a relatively small subcatchment of the Meuse river with a catchment size of 340 km^2. The catchment is partly located in Belgium (Walloon Region - 42%), where the Geul originates in Lichtenbusch, the Netherlands (South Limburg - 52%) and Germany (6%) (Klein, 2022). After a flow path of 56 km, the Geul joins the Meuse at Meerssen, around 7 km north of the city of Maastricht. The main

tributaries are the Gulp, Eyserbeek, and Selzerbeek, Figure A.2 of Appendix A illustrates that the three tributaries all join the Geul relative close to each other.

The Geul catchment has a distinctive hilly landscape with topographical features that are unique for the Netherlands. The river itself descends from approximately 360 meters at its source to 50 meters at its confluence with the Meuse. With an average slope of 3%, the Geul is considered a fast-flowing river by Dutch standards. As shown in Figure A.2, the gradient is not uniform. The river is steeper in the upstream area (0.02 m/m) than near the outlet (0.0015 m/m)(van Winden et al., 2014). The Belgian part is situated on a plateau and the river is less incised in the area compared to the Dutch part. In the Netherlands, the Geul valley is deeply incised in the surrounding plateaus. The valley is asymmetrical, with steep slopes on the eastern side and more gentle slopes on the western side (de Moor and Verstraeten, 2008). The floodplains are relatively large, with a width between 200 and 400 meters.

According to the Köppen-Geiger climate classification system, the area has a temperate oceanic climate of Cfb (Peel et al., 2007). This climate is characterized by the absence of a dry season, moderate temperatures, and warm summers (Van de Westeringh, 1980). The catchment is described as energy limited, which means that evaporation is limited by the available energy (e.g., from sunlight) and not by the availability of water (Gerrits et al., 2009). The average annual precipitation ranges from 720 mm near Meerssen (downstream) to 940 mm near Vaals (upstream part of the Netherlands). On average, the highest rainfall occurs in August (approximately 90 mm/month), while April receives the least precipitation (approximately 45 mm/month). Although rainfall intensity peaks during summer, flooding occurs predominantly in winter due to higher soil saturation (Klein, 2022)

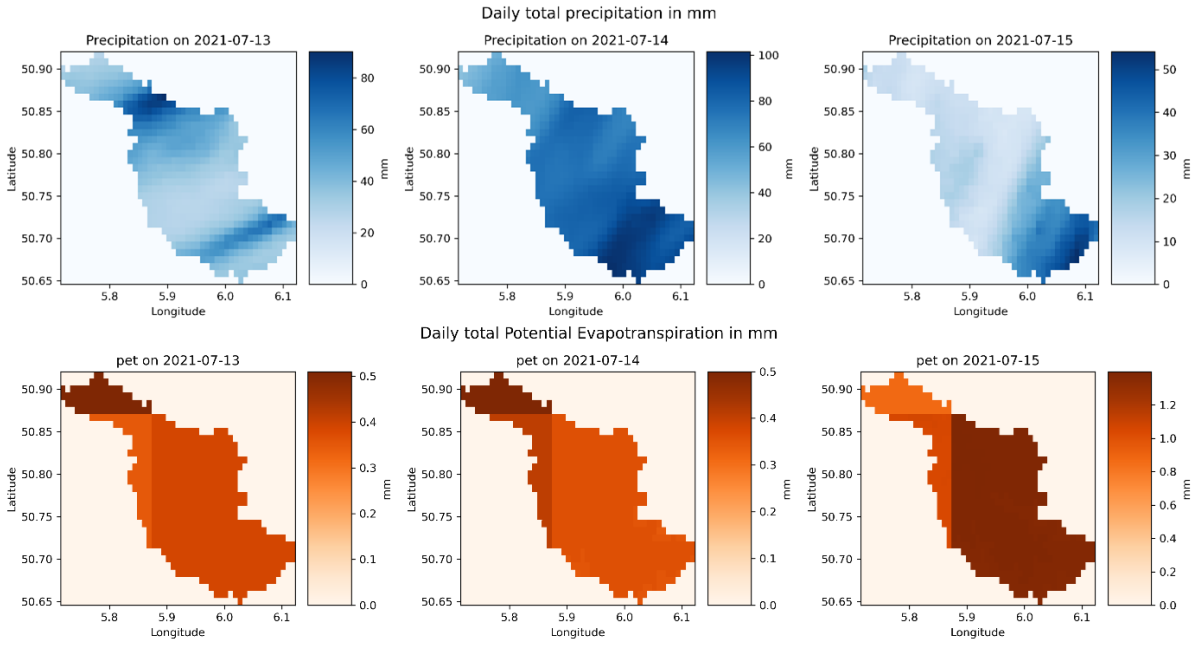

Figure 2.3: Rainfall during the 2021 event based on KNMI reanalysis radar data ; potential evapotranspiration during the 2021 event based on ERA5 radar data

The total rainfall during the 2021 event (13–15 July) was exceptionally high - cumulative precipitation over these three days exceeds the total monthly rainfall typical observed in the wettest month of the year. In contrast, potential evapotranspiration values are extremely small compared to precipitation, indicating that evaporation played an almost negligible role in the water balance during this event.

2.3. Hydrogeology and soils

In the Belgian and the southern part of the Netherlands, the Geul River is incised into rocks, such as sandstones, slates, and limestones. In the Dutch part downstream, the river is mainly cut into Creta-

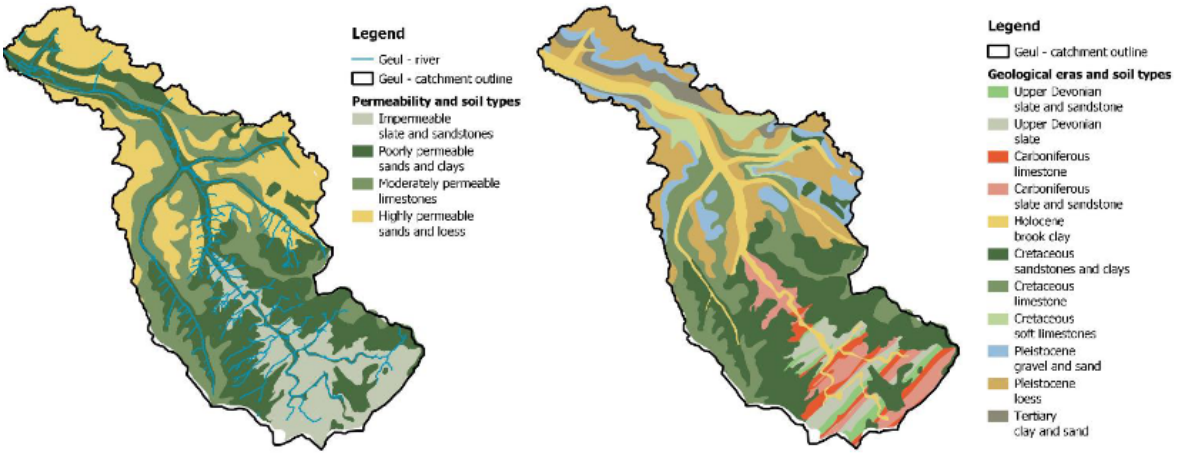

Figure 2.4: Geological overview of the Geul catchment. The map on the left shows a coarse classification of geological soil types according to their permeability (note that this refers to the parent material). The map on the right presents the distribution of geological formations by era (adapted from Bureau Stroming, 2022)

ceous lime and sandstones (de Moor and Verstraeten, 2008). Then a large part of the catchment is covered with fertile loess (silt-sized sediment), which was deposited during the Pleistocene (Bureau Stroming, 2022). In the Dutch part, soils are thick and characterized by moderate permeability, resulting in high water storage capacity and no Hortonian overland flow (Bouaziz, 2021). In contrast, in the Belgium part, soils are thinner and laying on impermeable rock and therefore can store less water (Bureau Stroming, 2022). The plateaus are defined by coarse silty(loess in Figure 2.4) or sandy soil texture, whereas the river valleys and floodplains have a loamy texture with higher clay content in the subsoil (Van de Westeringh, 1980).

Klein, 2022 found that during the 2021 flood event, groundwater monitoring wells in the catchment showed different response times and drainage behaviors, indicating high lateral porosity and matrix flow and the existence of complex hydrogeology in the catchment with significant groundwater storage in a deep aquifer system.

2.4. Stream characteristics

The Geul is one of the few rivers in the Netherlands without a stabilized riverbed, which allows it to meander freely through the landscape. In the past, parts of the river were straightened, which led to higher peak discharges (Van de Westeringh, 1980 ; Penning et al., 2024). More recently, meanders have been restored to increase natural water storage capacity. The drainage network is well developed in the upstream Belgian section, with a drainage density of about 13.5 m/ha, indicating a rapid hydrological response (de Moor et al., 2008). In contrast, the network is poorly developed in the lower Geul catchment and its tributaries (Gulp, Eyserbeek, Selzerbeek), with an average density between 4 and 5.6 m/ha (de Moor et al., 2008). This pattern suggests a good surface infiltration and water storage capacity in the Dutch part.

The average discharge of the Geul is approximately 2.8 m^3/s, however as the Geul is a rain-fed river the discharge is highly variable ranging from 1 m^3/s during dry periods to more than 40 m^3/s after a storm event (Klein, 2022).

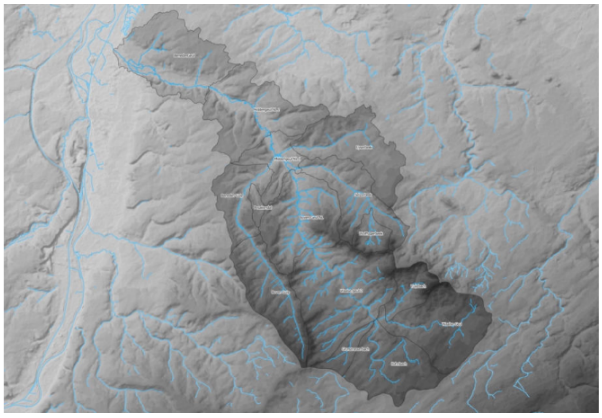

Figure 2.5: Stream network of the Geul catchment and its surrounding area (van Winden et al., 2014)

2.5. Land use and human influence

Land use in the catchment is largely determined by the topography of the terrain. The river valley consists mainly of grasslands, while the gentle slopes are a mix of grasslands and arable land. Steep slopes are covered with mixed forests and plateaus are used mainly for pastures. As shown in Figure 2.6, urban areas are concentrated around Kelmis, in the Eyserbeek tributary, and in Valkenburg and Meerssen.

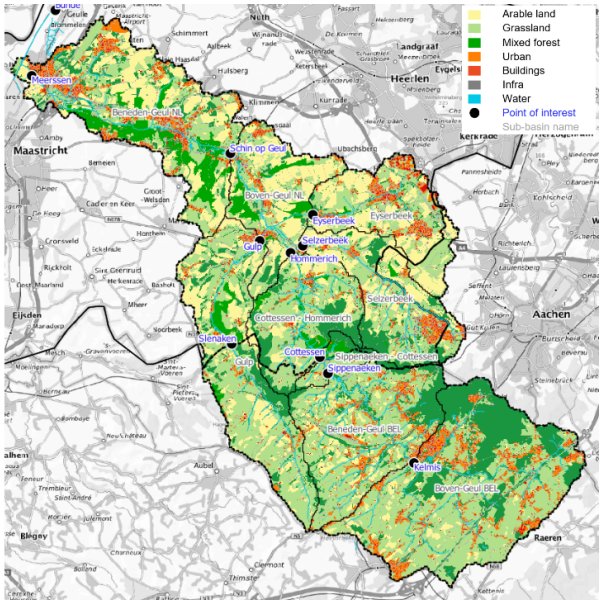

Figure 2.6: Land use in the Geul catchment (Slager et al., 2022)

The catchment area is the most densely populated in the Dutch region. Pastures dominate in the upstream catchments (Boven Geul België, Beneden Geul België, and Boven Geul Nederland), while arable land is more common downstream. The Geul catchment area serves multiple functions, including providing ecological environments, reservoirs for local drinking water, and flood control retention areas (de Moor et al., 2008). Tourism is a major industry for cities and villages in the river valley, particularly for Valkenburg.

2.6. Flood risk management

As the river is largely free to meander within its wide floodplains, only near the cities of Valkenburg and Meerssen is the riverbed stabilized, where a levee system locally confines the channel. In the Netherlands, the primary flood defenses along the major rivers are managed by Rijkswaterstaat and

financially supported by the government with safety standards ranging from 1 / 100 to 1/10 000 year failure probability (Ministerie Infrastructuur en Waterstaat, 2022). For tributaries, flood defenses are often not present or have significantly lower protection standards. In the urban areas of South Limburg, protection standards have a failure probability of 1 in 25 years (Strijker et al., 2023). In the past 20 years, the Water Board of Limburg has constructed several rainwater buffers, which are often integrated into the landscape, such as in valleys or tributaries of the Geul, dry valleys (valleys without permanent streams), and on slopes in the higher elevated areas (Deltares, 2023)

2.7. Summary of catchment key characteristics

Characteristic	Description / Value
Catchment area	~ 340 km^2
Main river length	~ 56 km
Source location	Lichtenbusch (Belgium–Germany border)
Outlet	Confluence with the Meuse River at Meerssen
Tributaries	Gulp, Selzerbeek and Eyserbeek
Elevation range	50 - 360 m
Dominant land use	Agricultural (pastures and arable land)
Discharge regime	Pluvial
Mean annual precipitation	~ 720–940 mm/year
Mean discharge	~ 2.8 m^3/s at Meerssen
Peak discharge (July 2021 event)	~ 135 m^3/s at Meerssen (Strijker et al., 2023)
Soil and geology	Mostly loess and clay covering sandstone and limestone formations

Table 2.1: Summary of catchment key characteristics

3

Conceptual Framework

This chapter provides the theoretical background necessary to understand the research approach presented in this thesis. Introducing the concept of rural nature-based solutions and, more specifically, the primary sponge function that is central in this study. Next, the dominant hydrological processes that control the primary sponge function are briefly described, with an emphasis on how soil hydraulic properties affect infiltration, available storage, and flow in the unsaturated zone. Finally, the chapter explains how these processes are represented in the two used hydrological models, providing a knowledge foundation for the event-based model study described in the methodology in Chapter 4.

3.1. The concept of rural NbS and primary sponge function

NbS are defined as “actions that protect, sustainably manage, and restore natural or modified ecosystems to address societal challenges effectively and adaptively, simultaneously providing human well-being and biodiversity” (IUCN, 2022). Although widely applied in urban stormwater management (Muishout, 2023), their catchment-scale flood mitigation potential is less frequently quantified and is frequently based on expert judgment rather than process-based modeling (Rogger et al., 2017).

Figure 3.1: The concept of nature-based solutions incorporated by the European Commission (European Commission, 2015).

As stated in Section 1.1, this study focuses on *rural NbS* that enhance the *sponge function* of the soil column. Because the term ’sponge function’ remains broad, here the emphasis is on the ability of the

soil to absorb and temporarily retain water, called the *primary sponge function* . Increasing this function means that a greater portion of rainfall infiltrates into the soil and is stored within it, thereby reducing and delaying runoff towards the stream network.

Several rural NbS can enhance the primary sponge function, including agroforestry, reforestation, cover cropping, reduced tillage, and wetland restoration. Agroforestry, for example, increases infiltration and water storage capacity by improving soil structure through root development(Calder et al., 2003) and by adding organic matter from leaf litter and surface residues (Ilstedt et al., 2016; Muys et al., 2021). Similarly, reforestation and cover cropping protect the soil surface, reduce compaction, and enhance porosity, while wetland restoration promotes temporary water storage and groundwater recharge. Collectively, these measures strengthen the primary sponge function of rural landscapes and thereby improve resilience to hydrological extremes (Ruangpan et al., 2020).

3.2. Soil-water processes governing the primary sponge function

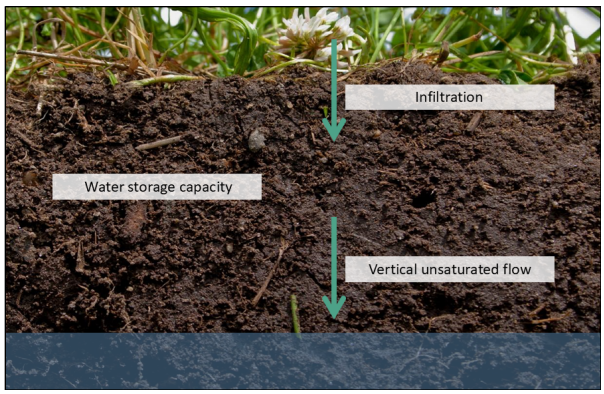

Figure 3.2: Focused soil-water processes

The primary sponge function of soil - defined by its pore structure, organic matter content, and hydraulic properties - controls how much rainfall contributes to immediate runoff versus delayed subsurface flow to the stream network. Rural NbS enhance this function by improving soil permeability, increasing organic matter, and creating deeper and more connected pore spaces. These changes result in greater vertical unsaturated flow and thereby infiltration and an increased water storage capacity within the soil column. Consequently, this study focuses on the *infiltration rate*, *vertical unsaturated flow*, and total *water storage capacity* as key soil-water processes to represent the effects of rural NbS.

3.3. Soil-water processes within the used models

In this study, hydrological models were used to investigate processes and scenarios. Given the event-based nature of this study, modelling is the only viable method to investigate and quantify the influence of soil-water processes on flood generation and mitigation. In addition to this, hydrological models make it possible to study the underlying processes that cannot be observed easily at the catchment scale. In this research, the plot-scale SWAP model is used to study detailed soil-water processes and its underlying soil hydraulic properties, while the distributed wflow$_{sbm}$ model is used to simulate catchment-wide responses.

3.3.1. SWAP model

General

The Soil–Water–Atmosphere–Plant (SWAP) model is a physically based, one-dimensional model. SWAP is an integrated model that describes the unsaturated zone and in part in the upper groundwater (Soil-Water) in relation to meteorological (climate) data (Atmosphere) and crop uptake and crop growth (Plant). It was developed by Wageningen University in the Netherlands and is used for a variety of applications, including irrigation management (Jiang et al., 2016), land use planning (Bonfante and Bouma, 2015), and modelling overland flow (Gusev et al., 2011). The SWAP model takes into account

various soil properties (texture and structure) and soil hydraulic properties, as well as plant characteristics, such as root growth and water uptake (Heinen et al., 2024). A summary of the input data used by the SWAP model can be found in Appendix B.

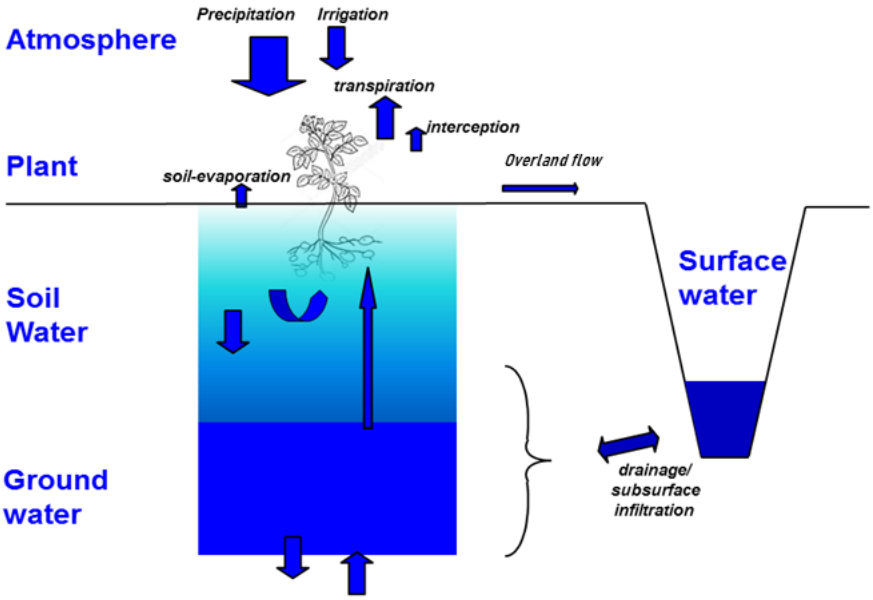

Figure 3.3: Swap model domain and the different fluxes (Adjusted from Kroes et al., 2017)

Soil module in SWAP

The core of the SWAP-model pertains to the water balance in the unsaturated – saturated top part of the soil. It solves the Richards equation (Richards, 1931) given here as

$$\frac{\partial \theta(h,t)}{\partial t} = \frac{\partial}{\partial z}\left(K(h,t)\left(\frac{\partial h(t)}{\partial z} + 1\right)\right) \tag{3.1}$$

where h is the pressure head with h ≥0 when the soil is saturated and h < 0 when it is unsaturated (cm), θ is the volumetric water content (cm^3/cm^3), K is the hydraulic conductivity (cm/d), z is the vertical coordinate (cm ; positive upward), the term 1 accounts for gravity (cm/cm), and t is the time (d).

The Richards equation is solved numerically for specific boundary conditions at the top (determined by the atmosphere) and at the bottom, for given relationships between h, θ, and K. The three variables h, θ, and K are related to each other. The relationship θ(h) is the water retention function and K(h) is the hydraulic conductivity function. These functions can be determined by measuring it on the field by using a tension infiltrometer or other equipment (Allaban, 2025) . But it appears that such data can be well described by analytical expressions. SWAP uses the relationships given by van Genuchten, 1980 for the water retention function, given by

$$S(h) = \frac{\theta(h) - \theta_{res}}{\theta_{sat} - \theta_{res}} = \begin{cases} 1, & 0 \le h \\ (1 + |\alpha h|^n)^{-m}, & h < 0 \end{cases} \tag{3.2}$$

Based on the hydraulic conductivity theory of Mualem, 1976 ; van Genuchten, 1980 derived the following expression for hydraulic conductivity

$$K(h) = \begin{cases} K_{sat}, & 0 \le h \\ K_{sat}\left(\frac{\left((1+|\alpha h|^n)^m - |\alpha h|^{n-1}\right)^2}{(1+|\alpha h|^n)^{m(Lexp+2)}}\right), & h < 0 \end{cases} \tag{3.3}$$

where S is the effective degree of saturation (dimensionless; [0 - 1]), θ_{res} is an asymptotic residual water content (cm^3/cm^3), θ_{sat} is θ at saturation (cm^3/cm^3), Ksat is K at saturation (cm/d) and α (cm), n, m and, Lexp (all three dimensionless) are shape parameters.

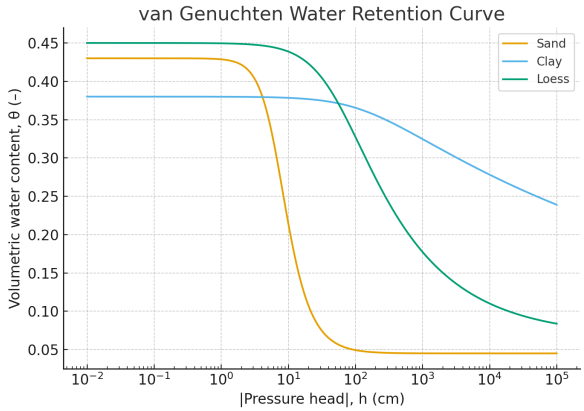

Figure 3.4: Water retention curves for three different soil types based on the analytical 'van Genuchten' expression

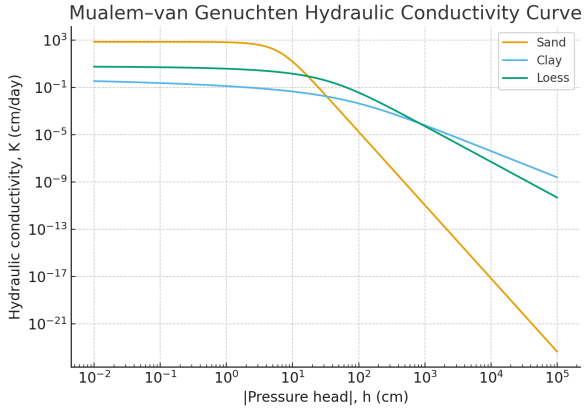

Figure 3.5: Hydraulic conductivity curves for three different soil types based on the analytical 'van Genuchten' expression (that is based on the Mualem expression)

Both relationships are shown in Figure 3.4 and 3.5. Showing the resulting curve for different soil types, thus different soil hydraulic properties. These relationships have been implemented in SWAP, for each soil layer the corresponding parameters θ_{res}, θ_{sat}, K_{sat}, α, n and L_{exp} should be supplied to run the model.

3.3.2. Wflow$_{sbm}$

General

The wflow$_{sbm}$ model is a distributed, grid-based hydrological model implemented in Wflow.jl. It represents water movement using bucket-type mass balance formulations for the unsaturated zone, groundwater, and surface runoff components. The wflow hydrological model framework was developed by the Deltares institute in the Netherlands. There are several models under the wflow shell, like wflow$_{hbv}$, wflow$_{topoflex}$ and wflow$_{sbm}$ (Schellekens, 2011). SBM stands for simple bucket model and the soil part of the wflow$_{sbm}$model has its roots in the Topog$_{SBM}$ model (Vertessy and Elsenbeer, 1999). Wflow_sbm is used for water resources management (Seizarwati and Syahidah, 2021), flood estimation (Laverde-Barajas et al., 2020), and ecohydrology impact assessments (Eulderink, 2019). The wflow$_{sbm}$ is a conceptual model that simulates the movement of water through a catchment using a combination of sub-models. These sub-models include the soil sub-model, a snow and glaciers sub-model, a rainfall interception by vegetation sub-model, a kinematic wave routing for surface and subsurface flow sub-model and a reservoirs and lakes sub-model. The schematic representation of the storages and fluxes within the different sub-models for an area without snowmelt and glaciers is shown in Figure 3.6a.

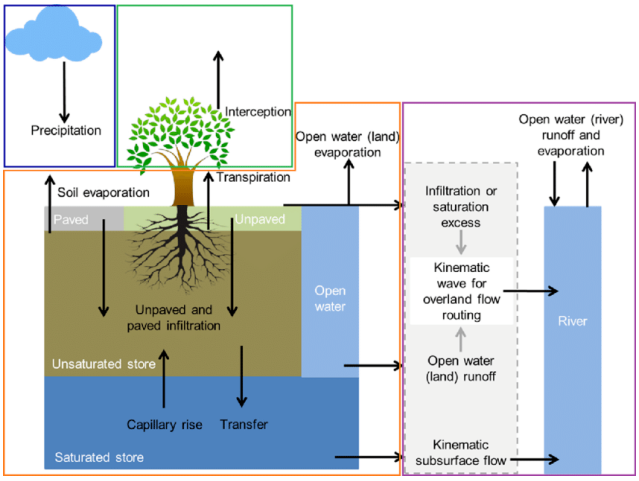

(a) Overview of the different fluxes in the wflow$_{sbm}$ model with the rainfall interception, soil, and kinematic wave sub-models highlighted (Schellekens, 2011).

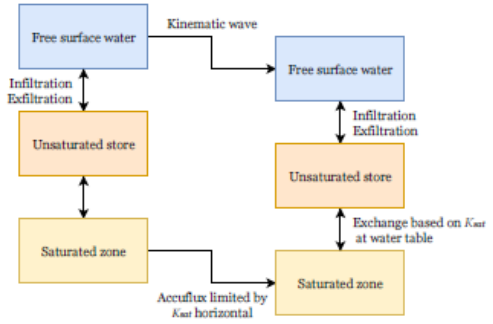

(b) Altered topog$_{SBM}$ soil module for wflow$_{sbm}$ (Van Verseveld et al., 2022).

Figure 3.6: Wflow$_{sbm}$ structure (left) and soil module (right)

Soil module in wflow$_{sbm}$

Vertessy and Elsenbeer, 1999 gave a detailed description of the Topog$_{SBM}$ model. The soil is considered as a bucket with a certain depth z$_t$ (mm), divided into a saturated store S (mm) and an unsaturated store U (mm). The top of the S storage forms a pseudo-groundwater table at depth z$_i$(mm) such that the value of S is given by

$$S = (z_t - z_i)(\theta_s - \theta_r) \tag{3.4}$$

where θ_s is θ_r at are the saturated and residual soil water contents, respectively.

The unsaturated store U is subdivided into storage U_s and deficit U_d. All infiltrating water enters the U store first, which is controlled by the $InfiltCapSoil$ infiltration parameter (mm/d).

$$\begin{aligned} U_d &= (\theta_s - \theta_r)z_i - U \\ U_s &= U - U_d \end{aligned} \tag{3.5}$$

The saturation deficit for the soil profile as a whole is defined as:

$$S_d = (\theta_s - \theta_r)z_t - S \tag{3.6}$$

The unsaturated layer is split-up in different layers, by providing the thickness (mm) of the layers. Using a unit head gradient , the transfer of water st (mm/d) from a U store to another U store layer is controlled by the vertical saturated hydraulic conductivity KsatVer mm/d at depth z (bottom layer) or z$_i$ (the depth of the pseudo-groundwater table), the effective saturation degree of the layer and the Brooks-Corey power coefficient (Brooks and Corey, 1964):

$$st = KsatVer\left(\frac{\theta - \theta_r}{\theta_s - \theta_r}\right)^c \tag{3.7}$$

C based on the pore size distribution (Brooks and Corey, 1964). Brooks–Corey and van Genuchten are equivalent parametric descriptions of soil hydraulic behavior. They both use a shape parameter for the pore-size distribution to reproduce a θ(h)- curve. In wflow$_{sbm}$, only the Brooks-Corey power coefficient is used.

3.3.3. Comparison of the soil-water processes

Table 3.1 outlines the fundamental differences between SWAP and wflow$_{sbm}$ in their approach to modelling soil-hydrological processes. SWAP relies on physical expressions including those by van

Genuchten-Mualem (VGM) to calculate soil water retention and conductivity curves, and solving Richards in a continuous manner (Heinen et al., 2024). In contrast, wflow$_{sbm}$ is based on a mass balance approach in combination with a Brooks–Corey power coefficient (Van Verseveld et al., 2024), offering a different depiction of vertical unsaturated flow.

Hydrologic process	**Approach in SWAP**	**Parameters in SWAP**	**Approach in wflow$_{\mathrm{sbm}}$**	**Parameters in wflow$_{\mathrm{sbm}}$**
Infiltration	Upper boundary of Richards' equation	VGM-parameters	Controlled by soil ratio and empirical infiltration parameter	InFiltCapSoil, InfiltCapPath, PathFrac
Vertical unsaturated flow	Richards' equation	VGM-parameters	Brooks–Corey equation	KsatVer, θ_r, θ_s, f_, c
Groundwater recharge	Bottom boundary of Richard's equation	VGM-parameters with Ksat,exp	Controlled by leakage parameter and Brooks–Corey transfer	KsatVer, θ_r, θ_s, c, MaxLeakage

Table 3.1: Summary of approaches and linked parameters in SWAP and wflow$_{\mathrm{sbm}}$ regarding the focused soil-related fluxes and storage. The full table is shown in Appendix C.

This conceptual difference is reflected in the parameterization: SWAP requires direct input of soil hydraulic parameters such as θ_{res}, θ_{sat}, α, n, and K_{sat} for the VGM-functions, while wflow$_{sbm}$ uses pedotransfer functions to link gridded soil- and land use-land cover maps to parameters such as InfilCapSoil, KsatVer, θ_r and θ_s. In addition, wflow$_{sbm}$ uses 'black box' parameters for calibration. For example, the depth decay parameter $f\_$ governs the exponential reduction of the saturated hydraulic conductivity with depth. The factor KSHF (shown in Table C.1) is a dimensionless multiplier that converts vertical saturated hydraulic conductivity to its horizontal counterpart for lateral groundwater flow. Both $f\_$ and KSHF are not measurable soil properties; rather, they are effective parameters that are usually estimated by calibration to match the simulated to the observed discharge.

Rural NbS modify soil and land cover properties, thereby altering hydrological stores and fluxes in addition to the targeted soil–water processes. These include interception, lateral subsurface flow, and overland flow. For the overall knowledge foundation, the approaches of the models are compared for these fluxes as well. Table C.1 provides a concise comparison of how all processes regarding the soil column are conceptualized in SWAP and wflow$_{sbm}$, and the parameters that govern their behavior.

4

Methodology

This study combined a physics-based plot-scale model (SWAP) and a distributed catchment-scale model (wflow$_{sbm}$) to investigate soil-water processes and the potential effects of rural NbS on flood mitigation. The methodology consisted of four main parts: (1) A parameter sensitivity analysis using SWAP to identify key soil-water parameters , (2) a hydrograph sensitivity analysis using wflow$_{sbm}$, (3) a rural NbS scenario development and (4) a rural NbS scenario assessment using wflow$_{sbm}$.

4.1. Research framework

The workflow implements a two-model chain that links plot-scale processes to catchment-scale responses for July 2021. This coupling propagates process understanding from local dynamics to catchment-scale river discharge modelling. All outputs are annotated with the corresponding research questions of section 1.5.

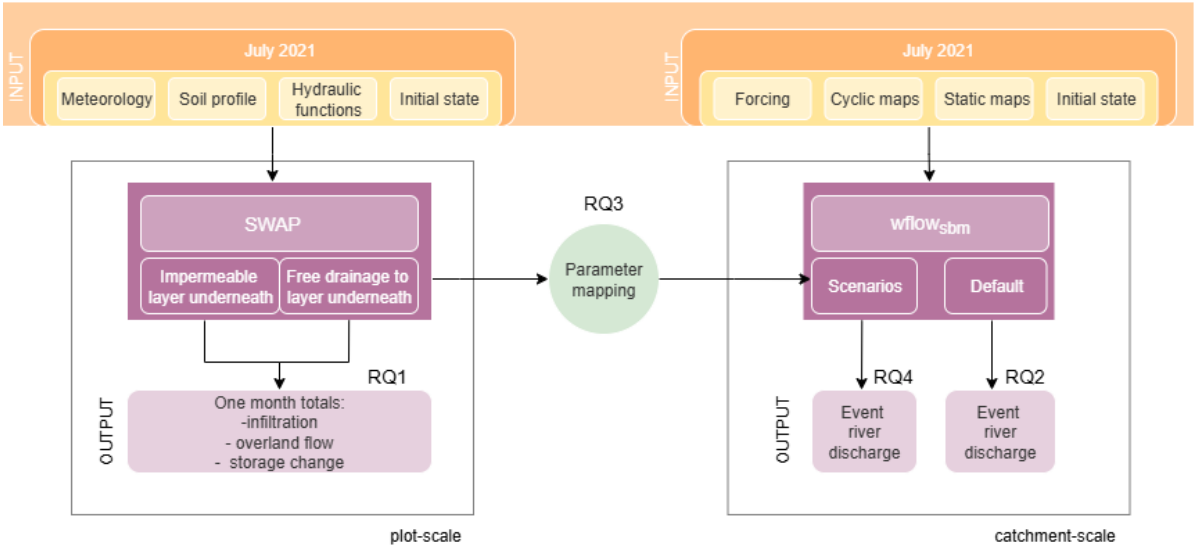

Figure 4.1: Methodology flowchart

4.2. SWAP, plot-scale

4.2.1. Model setup

The meteorological forcing consisted of precipitation, temperature, and potential evapotranspiration data from the Maastricht weather station for July 2021. In the model, no slope was imposed to mimic the topography of the plateaus. This resulted in a vertical water balance that focused on infiltration,

percolation, storage change, and overland flow generation.

The SWAP simulations used three representative soil profiles to capture the main soil types present in the Geul catchment: clay, sand, and loess (DinoLoket, 2025). Each profile was divided into two layers: a top layer representing the rooting zone and a sub-layer representing the sub soil. For clay, sand, and loess respectively, the (B11, B2, B14)-toplayer and (O13, O2, O14)-sublayer were chosen from the Staringreeks data.

All hydraulic properties - used for the VGM-equations (van Genuchten, 1980 ; Mualem, 1976) - were assigned to the top- and sublayer. Staringreeks data, which provide default soil hydraulic parameters per soil type (Heinen et al., 2022) were used. This setup allowed SWAP to simulate the dynamics of infiltration and soil moisture for the three types of soil and to evaluate how variations of the VGM parameters (θ_{res}, θ_{sat}, K_{sat}, α, and L_{exp}) affect the partition of infiltration-overland flow under the extreme rainfall event of July 2021.

4.2.2. Sensitivity analysis

An univariate sensitivity analysis was performed by scaling key soil parameters over realistic ranges to assess their effect on infiltration and overland flow generation. Specifically:

- θ_{res}, θ_{sat}, K_{sat}, α, and L_{exp} were varied between 0.5–1.5 times its default value.
- To mimic the soil profile's lower boundary, two bottom-boundary conditions were simulated: (i) free drainage implemented as a unit hydraulic gradient , and (ii) an impermeable base implemented as a zero-flux lower boundary . The free drainage scenario represents the deep groundwater tables (Klein, 2022) that are present in the catchment. The impermeable scenario represents the low-permeability sandstone layers below the top- and subsoil that are also present in the catchment (de Moor and Verstraeten, 2008).
- The resulting cumulative infiltration, soil moisture storage, and overland flow after one month (1-31 July 2021) were analyzed by magnitude and to identify the most influential VGM-parameters.

The SWAP results of the free drainage scenario were also used to derive soil parameters that served as a proxy for the rural NbS, which were later mapped to the wflow$_{sbm}$ model (see Figure 4.1).

4.3. Wflow$_{sbm}$, catchment-scale

A pre-calibrated wflow$_{sbm}$ model for the Geul catchment (Klein, 2022) was used as the default model. The overview of all the possible states, fluxes and parameters of the simple bucket model are listed in Appendix B.

Initial conditions

The model needs a file which provides the model's state initial conditions. The file was generated by running a spin-up simulation from 2019 until 1 July 2021, ensuring that the model state variables (e.g., saturated soil store, unsaturated soil store) were in equilibrium before the start of the main simulation period.

Spin-up period

The choice of timestep for the spin-up period proved to be crucial. Initial tests using a 6-hourly timestep, resulted in a soil profile that was significantly less saturated at the start of July 2021. This is illustrated in Appendix B, where the unsaturated storage of the hourly spin-up is visibly lower compared to the 6-hourly spin-up. The difference is likely caused by a large rainfall event that occurred at the end of June 2021 (Figure 4.2). At a 6-hour resolution, rainfall peaks may not have been represented with sufficient temporal detail, reducing infiltration and leading to an unrealistic dry catchment. Using an hourly timestep for the spin-up period resulted in a more realistic and spatially heterogeneous distribution of soil moisture states at the start of the simulation period.

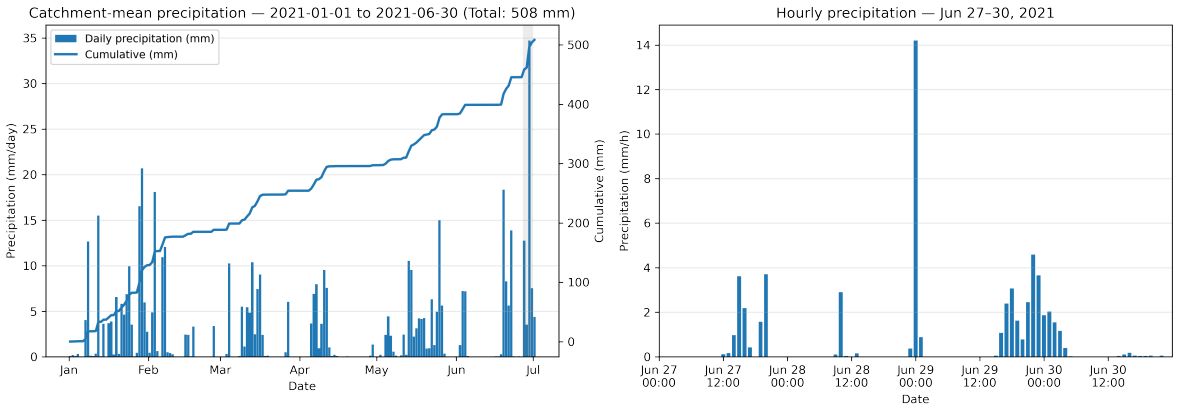

Figure 4.2: (Cumulative) Rainfall during last year of spin-up period (left) ; Zoomed-in on the last days before the beginning of the simulation period

Cyclic forcing

The cyclic input contains the hourly forcing data consisting of precipitation, potential evapotranspiration, and temperature. ERA5 is the fifth generation ECMWF (European Center for Medium-Range Weather Forecasts) reanalysis for global climate and weather. The original 0.25 ° x 0.25 ° (approximately 31 km^2) hourly precipitation data set has been scaled up) to match the grid size of the model of ≃ 0.57 km^2 (Hersbach et al., 2020).

The Static input

The static input for the model includes the Digital Elevation Model, river gridcells, land use - land cover map (LULC) and all the static parameters. The (LULC) that was used for these simulations is the Corine Land Cover Map 2018, which has a 300 m^2 resolution. Some static parameters that have their influence on the soil column are shown in Figure 4.3.

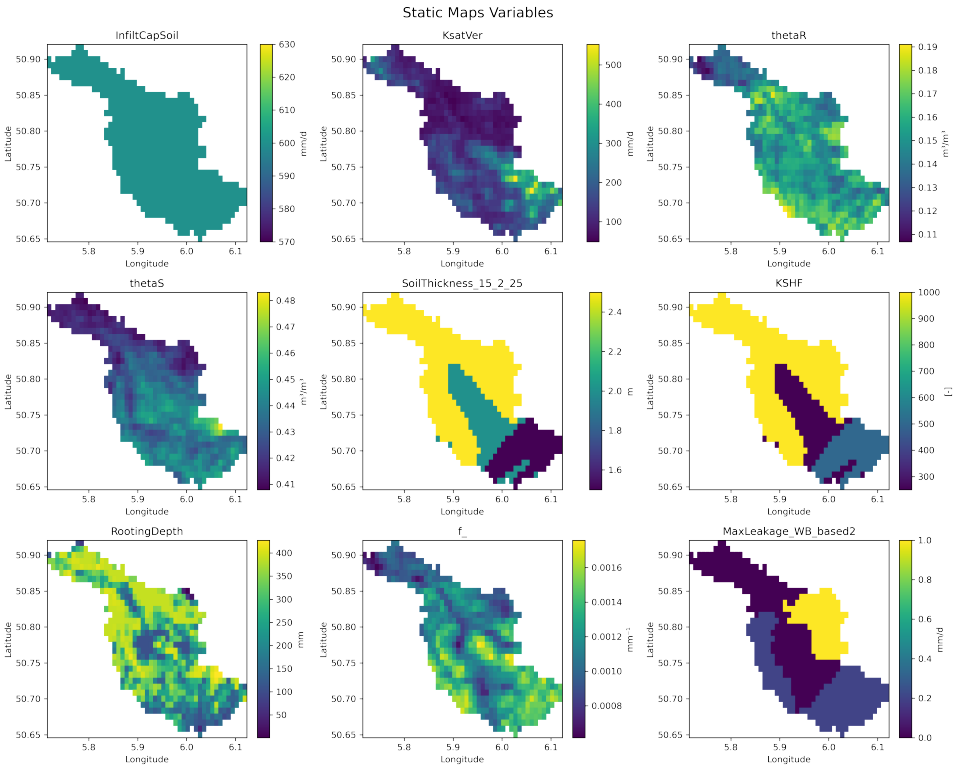

Figure 4.3: Spatial distribution of static soil variables used in the wflow$_{sbm}$ model for the Geul catchment.

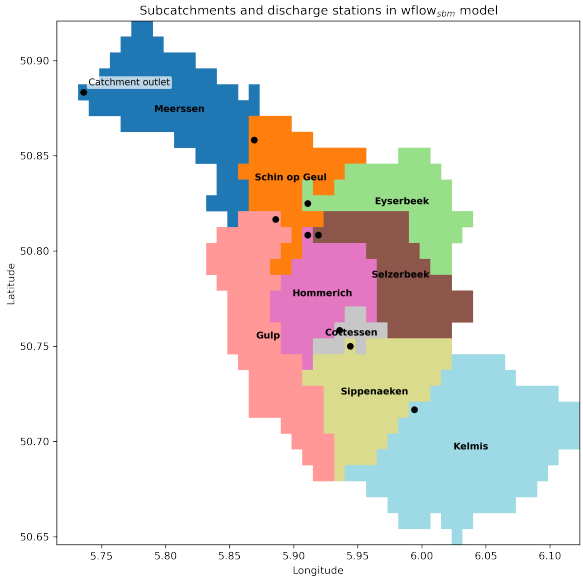

Figure 4.4: Setup of the subcatchments and discharge stations in the model ; Gulp, Selzerbeek and Eyserbeek being the tributaries.

Model structure

The wflow$_{sbm}$ model has been set up with a resolution of 0.00833 ° (or approximately 600m x 925 m). Nine discharge gauges —Kelmis, Sippenaeken, Cottessen, Hommerich, Gulp, Selzerbeek, Eyserbeek, Schin op Geul, and Meerssen — were included on the static maps. Subcatchments were delineated automatically from the digital elevation model using the local drainage direction network, assigning one outlet per gauge and resulting in nine subcatchments (Figure 4.4). It was run with time steps of an hour, to get the temporal variations of the rainfall and be able to analyze the temporal variations of the discharge.

4.3.1. Hydrograph sensitivity analysis

A parameter sensitivity analysis was performed to identify the soil-related model parameters that most strongly influence the simulated river peak flows during the flood event. The parameters considered in the analysis are shown in Figure 4.3 and summarized in Table 4.1. Each parameter was scaled between 0.5 and 1.5 times its baseline value to assess its effect on the model output.

Parameter	Unit	Model Value Range	Mean Model Value	Scale Factor	New SWAP-Based Value
InfiltCapSoil	mm/d	600	600	0.5 – 1.5	125
KsatVer	mm/d	48 – 552	151	0.5 – 1.5	127
$f\_$ parameter	–	0.0008 – 0.004	0.0012	0.5 – 1.5	–
KsatHorfrac	–	250 – 1000	747	0.5 – 1.5	–
θ_s	m/m	0.4 – 0.5	0.43	0.5 – 1.5	0.42
θ_r	m/m	0.1 – 0.3	0.15	0.5 – 1.5	0.02

Table 4.1: Overview of key soil parameters used in the model, including their ranges, mean values, applied scale factors for sensitivity anal, and new values used in sensitivity analysis.

The effect of each parameter adjustment was assessed by analyzing the resulting hydrographs and evaluating:

- **Peak discharge magnitude:** change in maximum simulated discharge relative to the default model.
- **Timing of peak discharge:** difference between simulated peak timing and default model.
- **Fit to observations:** visual comparison of simulated and observed hydrographs at the gauge stations.

This step allowed the identification of the most influential parameters controlling flood peak magnitude and timing under the 2021 July conditions and one-by-one comparison between the SWAP-based value and the default model's value. This is directly related to research question 2.

4.3.2. Rural-NbS scenario development

Using the insights gained from the SWAP results from section 5.1, the hydraulic soil properties of sand were combined to represent rural NbS. All wflow parameters that could be mapped by a SWAP-value were modified, and thereby answering research question 3. This resulted in modifications of the four combined key parameters listed in Table 4.2, ensuring a realistic representation of infiltration capacity, vertical unsaturated flow, and effective water storage capacity. The mapping conversions were as follows:

- InfiltCapSoil [mm/day] = topsoil Ksat [cm/day] x 10
- KsatVer [mm/day] = subsoil Ksat [cm/day] x 10
- $\theta_s = \theta_{sat}$
- $\theta_r = \theta_{res}$

Parameter	Unit	Default model value range	Mean default model value	Rural NbS scenario
InfiltCapSoil	mm/d	600	600	125
KsatVer	mm/d	48 – 552	151	127
θ_s	m/m	0.4 – 0.5	0.43	0.42
θ_r	m/m	0.1 – 0.3	0.15	0.02

Table 4.2: The modified model parameters that combined result in the rural NbS scenario.

4.3.3. Rural-NbS scenario assessment

These were implemented in wflow$_{sbm}$ in three spatial scenario types:

- **Single-subcatchment scenarios:** Modified parameters were applied to the Boven Geul and Beneden Geul subcatchments individually to evaluate spatial variability in hydrological response.
- **Catchment-wide scenario:** Modified Parameters were applied to all unpaved areas to represent a theoretical upper bound for the implementation of rural NbS in the catchment.

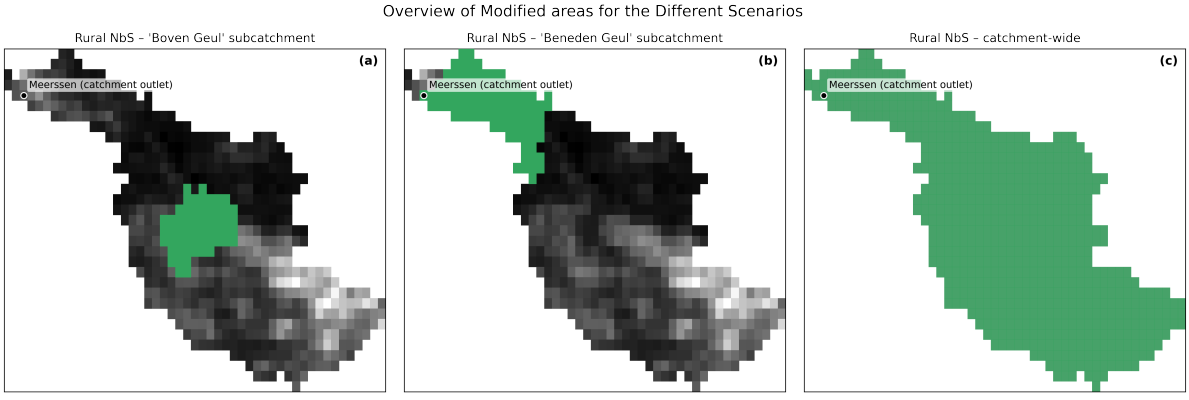

Figure 4.5: Overview of grid cells where soil hydraulic parameters were modified for the three rural NbS scenarios: (a) Boven Geul subcatchment, (b) Beneden Geul subcatchment and (c) catchment-wide. The displayed modifications only affect model results in grid cells classified as unpaved in the static maps.

The effect of each scenario was evaluated from the hydrographs by assessing peak magnitude, peak timing, and total runoff volume, thereby directly addressing Research Question 4.

5

Results

This section presents the results of the analyses conducted in this research. The results are organized into four parts: (1) A parameter sensitivity analysis performed with SWAP to identify the most influential VGM-parameters, (2) a hydrograph sensitivity analysis to soil parameters in wflow$_{sbm}$, (3) the effect of a rural NbS scenario applied in subcatchments, and (4) the effect of a catchment-wide rural NbS scenario on flood hydrographs with wflow$_{sbm}$.

5.1. SWAP, plot-scale

5.1.1. Sensitivity analysis

To better understand how the Van Genuchten–Mualem (VGM) parameters influence the primary sponge function of soils — expressed as the infiltration-to-overland flow ratio — a sensitivity analysis was conducted under the meteorological forcing of July 2021. The 3×3 subplot presents results for three soil types (Clay, Loess, Sand; rows) and three cumulative processes (Infiltration, Overland flow, Storage change; columns). For each type of soil, the parameters θ_{res}, θ_{sat}, K_{sat}, α, and L_{exp} were multiplied by factors of 0.5 and 1.5 relative to the empirical values for each type of soil. The dots indicate the cumulative values simulated after one month, while the dotted lines connect paired perturbations of the same parameter. Figure 5.1 illustrates the relative influence of the VGM soil hydraulic parameters on the water infiltration-overland flow ratio under free drainage conditions at the bottom boundary of the soil column.

In the simulations, the infiltration and overland flow processes were found to be more sensitive to the saturated water content θ_{sat} and the saturated hydraulic conductivity K_{sat} for the three types of soil. An increase in either parameter strongly enhanced infiltration and reduced overland flow, while a reduction had the opposite effect. In contrast, the cumulative storage change of sand and loess was particularly sensitive to the inverse of the air-entry value α, which controls the steepness of the soil water retention curve (van Genuchten, 1980).

In this scenario, the sand effectively absorbs all the rainfall minus evaporation, preventing any overland flow. This observation is logical, as the model lacks any topographical gradient, resembling a scenario where a significant amount of water is simply poured onto the sand. Under real-world conditions, the water would similarly just infiltrate the sand.

The scenario with an impermeable layer beneath the topsoil is presented in Figure D.2 (Appendix D). In general, its parameter sensitivities are comparable to those of the free-drainage scenario; the only notable deviation is the van Genuchten α parameter, which exhibits a distinctly different sensitivity pattern. This makes sense as : Under free drainage conditions, the soil column can transmit infiltrated water downward without restriction, making the α parameter (air-entry value) influential because it governs the vertical redistribution of water (Mualem, 1976). However, when an impermeable bottom boundary is imposed, infiltration becomes limited by the storage capacity of the soil rather than its redistribution dynamics. In this case, θ_{sat} dominates the storage change, as it directly determines how much water

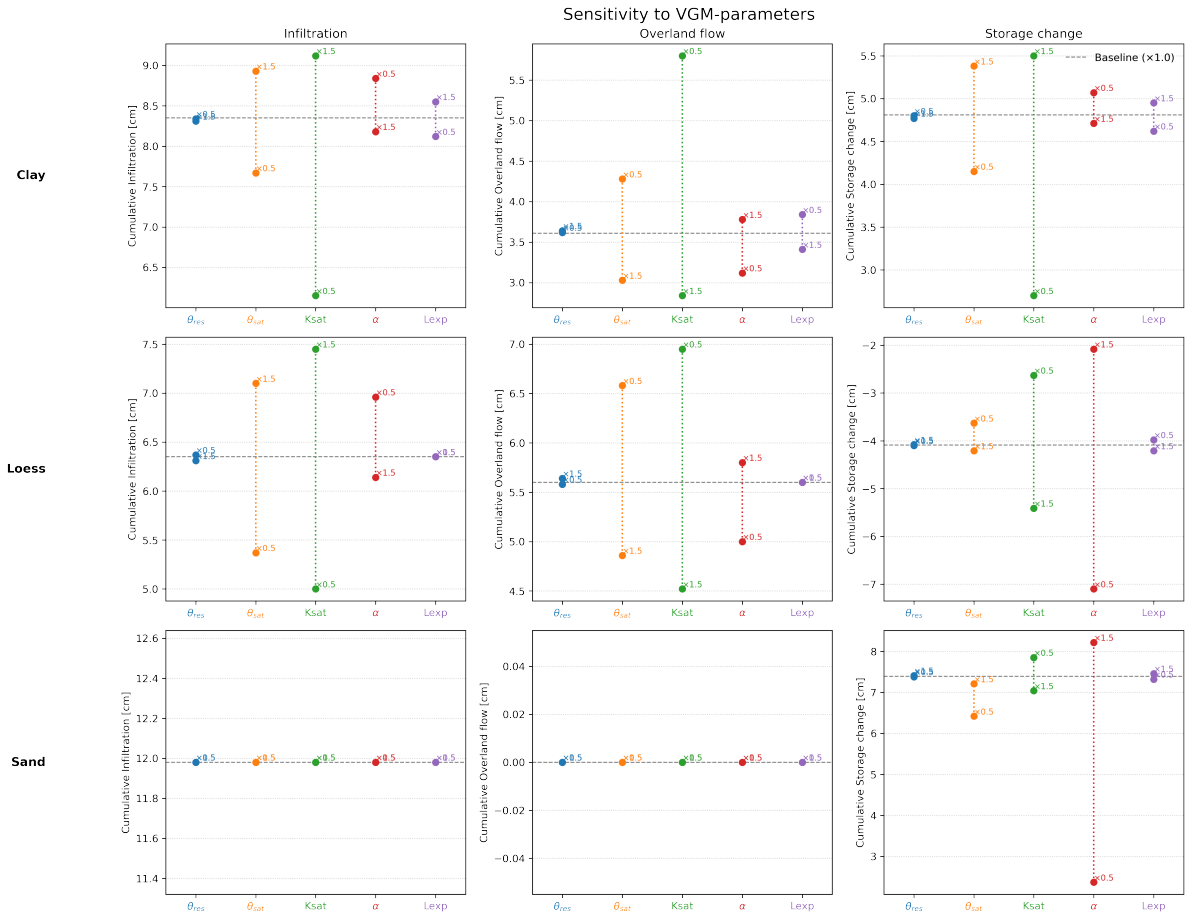

Figure 5.1: Sensitivity analysis of Van Genuchten–Mualem parameters on cumulative infiltration, overland flow, and storage change in the soil column, simulated with the SWAP model under free drainage conditions (July 2021).

can be stored. Although Ksat also determines the dynamics of redistribution, it is still influential here , as it still influences the infiltration rate on the soil surface.

In both free drainage and impermeable bottom boundary scenarios, sandy soil exhibits the same behavior: it absorbs all rainfall (minus evaporation), leaving infiltration, overland flow, and storage change unaffected by parameter variations. Using sand's hydraulic properties can enhance cumulative infiltration by approximately 87.5% compared to Loess (which is a dominant soil layer in the catchment). This magnitude is consistent with published field studies and meta-analyses on rural NbS/land-use change: for example, a meta-analysis reports a $\simeq 84.17\%$ increase in steady infiltration when cropland is converted to agroforestry (Sun et al., 2018), with comparable gains documented in a meta-analysis for cover crops (Çerçioğlu et al., 2025) and alternative agricultural practices (Basche and DeLonge, 2019). Consequently, the resulting SWAP-derived parameter set is transferred to wflow$_{sbm}$ to simulate rural NbS as a proxy, as discussed in Sections 5.3.2–5.3.3.

5.2. Wflow$_{sbm}$, catchment-scale

To gain a better understanding of how the default wflow$_{sbm}$ model represents the hydrological response of the Geul catchment under the extreme conditions of July 2021, flood hydrographs were generated for all nine subcatchments. These simulated hydrographs were compared with observed discharge data obtained from Waterschap Limburg (2025) and plotted alongside the spatially distributed precipitation input for each subcatchment. Both simulated and observed discharges were normalized to facilitate direct comparison with the precipitation forcing, allowing a clearer assessment of the rainfall–runoff response.

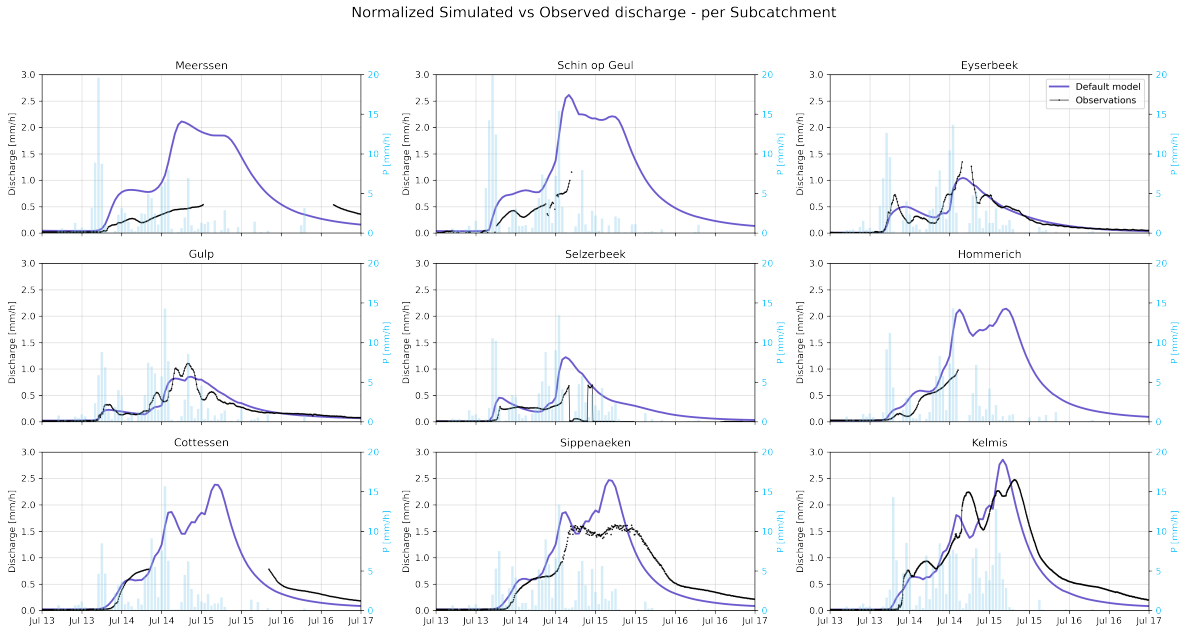

Figure 5.2: Simulated discharge from the default wflow$_{sbm}$ model (normalized) compared with observed discharge for each subcatchment during the July 2021 flood event, shown alongside subcatchment precipitation forcing.

Figure 5.2 shows the comparison between simulated discharge from the default wflow$_{sbm}$ model and the observed discharge data for the July 2021 flood event, together with precipitation forcing per subcatchment. In general, the model reproduces the timing and magnitude of the flood wave reasonably well in the upstream subcatchments and the tributaries(Selzerbeek, Gulp and Eyserbeek). However, in the middle and downstream subcatchments (e.g., Meerssen), simulated peaks tend to occur too early and are often overestimated. This behavior suggests that the current parameterization underestimates the natural retention capacity — the “primary sponge function” — of the soils in these areas, resulting in a flood wave that is too sharp and timed too early. The observed hydrographs indicate that the catchment already exhibits a strong natural buffering capacity downstream of Cottessen, which is not fully captured by the current model setup.

Consequently, when evaluating rural NbS scenarios that aim to improve infiltration and soil water storage, the location of implementation becomes critical. Understanding how the model’s baseline infiltration and storage parameters influence the hydrological response of each subcatchment is therefore a crucial step before interpreting scenario results. Therefore, the following section systematically assesses the sensitivity of the simulated flood hydrographs to the key soil-water parameters described in Section 4.4.3.

5.2.1. Sensitivity of simulated flood hydrographs

Because the default model tended to overestimate peak flows in several subcatchments, this section examines the sensitivity of simulated hydrographs to soil-water parameterization. Key parameters were multiplied by factors of 0.5 and 1.5, and — where possible — replaced with values mapped from SWAP to wflow$_{sbm}$. Together, these analyses highlight the key parameters most strongly controlling flood magnitude and timing.

Because the default infiltration capacity (InfiltCapSoil) in wflow$_{sbm}$ was set very high to avoid generating Hortonian overland flow outside urbanized areas (Bouaziz, 2021), the simulated hydrographs show little sensitivity to changes of ± 50% (see Figure 5.3). The saturated hydraulic conductivity ($Ksat$) of the topsoil in SWAP is considerably lower than the default InfiltCapSoil used in wflow$_{sbm}$. Consequently, setting it to the SWAP-based value (125 mm/d) results in higher simulated peak discharges. But only

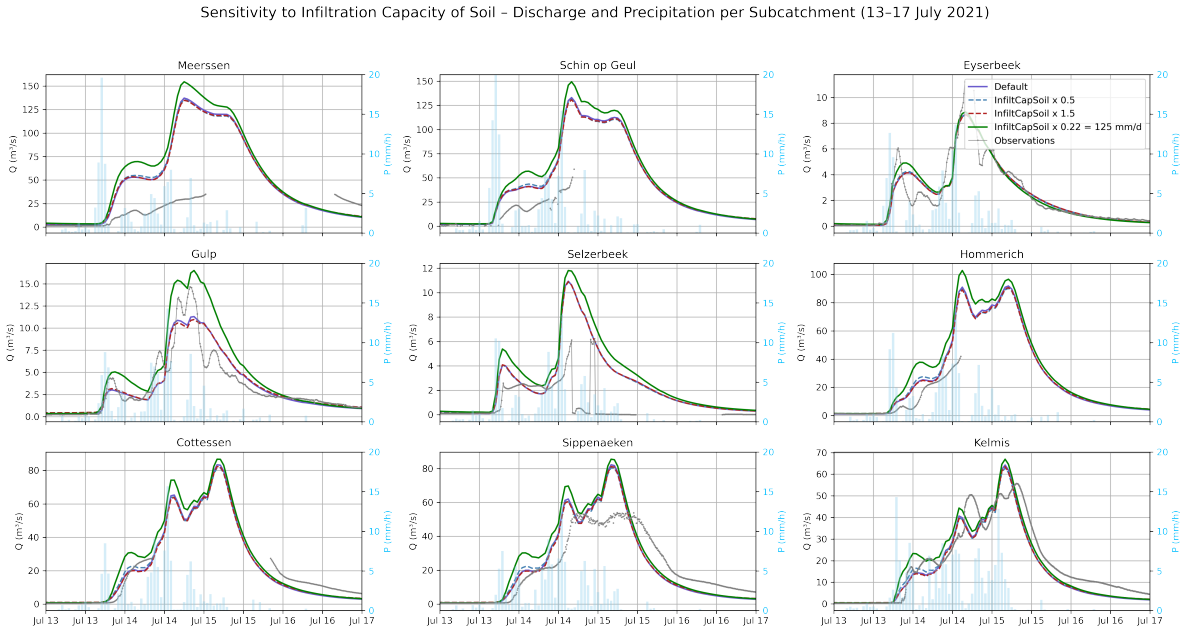

Figure 5.3: Simulated discharge sensitivity to infiltration capacity (InfilCapSoil) for nine subcatchments during the July 2021 flood event. Shown are the default model (purple), scenarios with InfilCapSoil × 0.5 (blue dashed), × 1.5 (red dashed), and set to 125 mm /d (green), with precipitation forcing (bars, right axis) and observed discharge (grey) where available.

for the Gulp it results in a substantial difference in discharge.

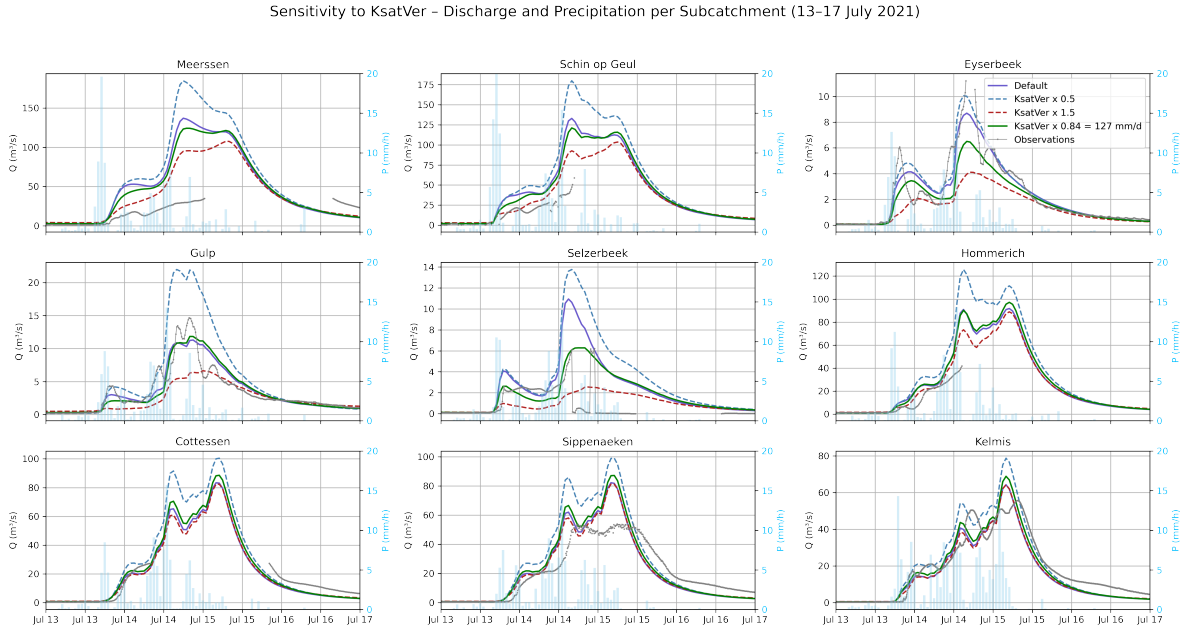

Figure 5.4: Simulated discharge sensitivity to saturated vertical conductivity (KsatVer) for nine subcatchments during the July 2021 flood event. Shown are the default model (purple), scenarios with KsatVer × 0.5 (blue dashed), × 1.5 (red dashed), and set to 127 mm /d (green), with precipitation forcing (bars, right axis) and observed discharge (grey) where available.

Scaling KsatVer shows a much stronger impact on the simulated hydrographs (Figure 5.4). Reducing KsatVer by half (blue dashed) substantially increases the simulated peak discharge in the downstream part and the tributaries. In contrast, increasing KsatVer by 50% (red dashed) lowers the flood peak and

even changes its shape.

Because KsatVer is highly heterogeneous across the catchment, replacing its default distribution with SWAP-derived values produces a spatially variable effect. In the Eyserbeek and Selzerbeek subcatchments, the default model uses relatively low KsatVer values, which limit infiltration and generate higher, quicker peaks. The SWAP-based values (127 mm/d) are higher in these areas, allowing more infiltration and resulting in lower and more attenuated peak discharges — particularly improving the fit for Selzerbeek. This local reduction in peak flows propagates downstream, leading to a slightly attenuated flood hydrograph at the catchment outlet (Meerssen, green line). Interestingly, this outcome is somewhat counterintuitive, as the SWAP-based KsatVer is actually lower than the mean of the default model (≈151 mm/d).

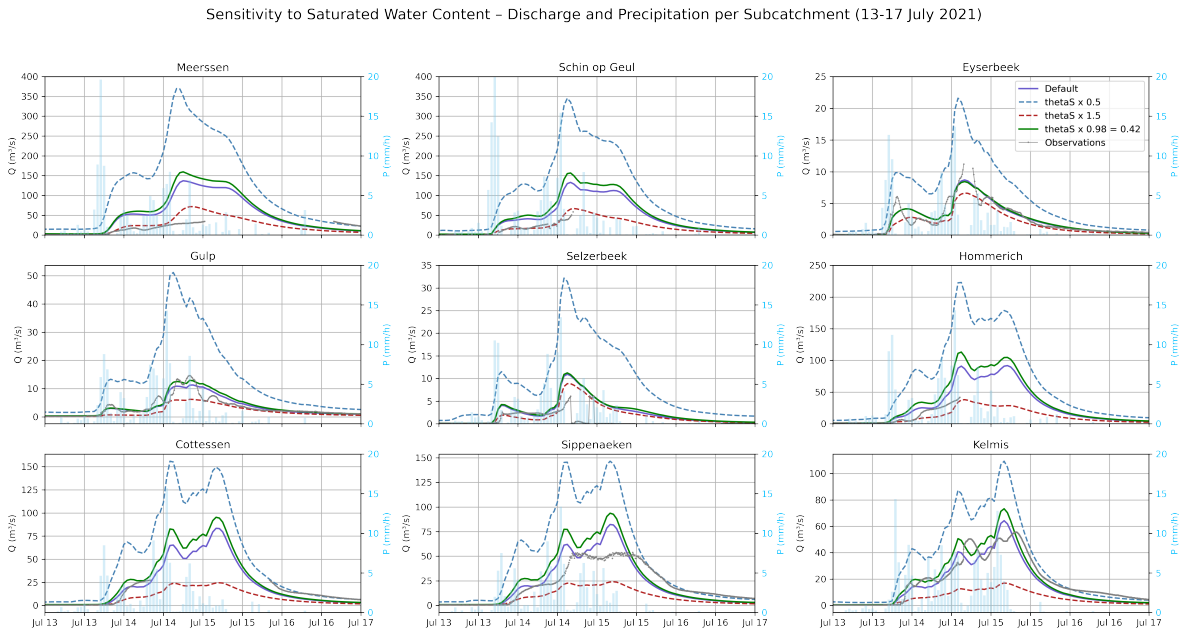

Figure 5.5: Simulated flood hydrograph sensitivity to saturated water content (θ_s) for nine subcatchments during the July 2021 flood event. Shown are the default model (purple), scenarios with θ_s × 0.5 (blue dashed), × 1.5 (red dashed), and set to 0.42 m /m (green), with precipitation forcing (bars, right axis) and observed discharge (grey) where available.

Unlike KsatVer, which had localized effects due to its heterogeneity, changes in θ_s shift the overall water balance more uniformly, affecting all subcatchments similarly Increasing θ_s by 50% (red dashed line) significantly lowers simulated peak discharges, especially at the more upstream subcatchments. While decreasing it by 50% (blue dashed line) produces unrealistically high peaks across almost all subcatchments. This confirms that θ_s strongly controls the available storage capacity and thus the runoff generation.

As shown in Figure 5.5, applying the SWAP-mapped θ_s affects the simulation differently across the catchment. While the SWAP-derived value (green line) generally increases the simulated flood peaks and leads to a poorer fit with observed discharges at most locations, it improves the agreement in tributaries such as the Eyserbeek and Gulp.

Another soil parameter assessed for its influence on the flood hydrograph was θ_r, the residual water content. As can be seen in Figure 5.6, this parameter shows a considerable effect on the shape of the flood hydrograph when scaled relative to its default value. However, further reductions in θ_r below $0.07\,\mathrm{m/m}$ do not result in significant changes. Notably, the flood hydrograph obtained using the SWAP-based value of $0.02\,\mathrm{m/m}$ is almost identical to that produced by $\theta_r \times 0.5$. Overall the plots suggest that lowering θ_r could be beneficial to fit the simulated hydrograph to the observations downstream of

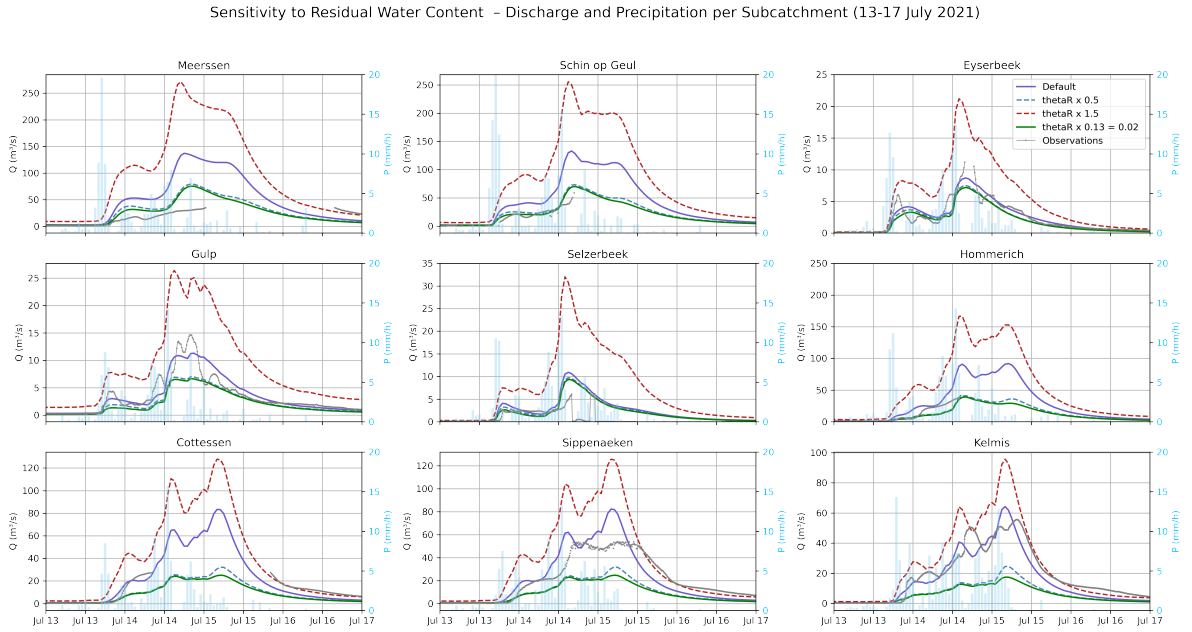

Figure 5.6: Simulated flood hydrograph sensitivity to saturated water content (θ_r) for nine subcatchments during the July 2021 flood event. Shown are the default model (purple), scenarios with θ_r × 0.5 (blue dashed), × 1.5 (red dashed), and set to 0.02 m/m (green), with precipitation forcing (bars, right axis) and observed discharge (grey) where available.

Cottessen.

In addition to the four key parameters discussed above (θ_s, θ_r, *KsatVer*, and *InfiltCapSoil*), the sensitivity analyses for the scaling parameter $f\_$ and the multiplier KSHF are presented in Appendix E. These parameters were not included in the main discussion because their default values are already extremely low ($f\_$) or high (KSHF), meaning that even substantial relative changes (±50%) resulted in very small differences in the simulated hydrographs. For completeness, the full set of 3×3 subplots for both parameters are provided in the Appendix.

Finally, Figure 5.7 summarizes the effect of individually applying SWAP-based parameter values on the simulated discharge for the entire catchment. The figure clearly demonstrates that not all SWAP-based parameters attenuate the flood peak, and the magnitude of their influence varies considerably. Among all soil parameters, θ_s (saturated water content) and θ_r (residual water content) have the most pronounced effects under extreme rainfall conditions. Reducing the mean θ_s by only 0.01 m/m leads to a substantially higher simulated flood peak and a 13% increase in the total event runoff volume. Conversely, lowering θ_r significantly reduces peak discharge and decreases the total runoff volume by almost 49%. In particular, θ_r is the only parameter that significantly alters both the shape of the hydrograph and the timing of the peak. This strong response is partly explained by the relatively low SWAP-based value compared to the mean value of the default model. These findings are consistent with the sensitivity analyses presented earlier, which also highlighted θ_s and θ_r as key controls on the downstream subcatchments.

5.2.2. Rural NbS-scenario applied in subcatchments

Because the Boven Geul subcatchment contains a large proportion of agricultural land that could potentially be converted to a sponge landscape, this area was selected for the first scenario analysis. SWAP-based parameter values were applied as a proxy for rural NbS to assess their effect on the timing and magnitude of discharge at the subcatchment outlet (Figure 5.8). The result indicates that a slight increase is observed in the overall simulated discharge. Although the result differs from the initially desired outcome, the findings are consistent with the sensitivity analysis, which showed that the

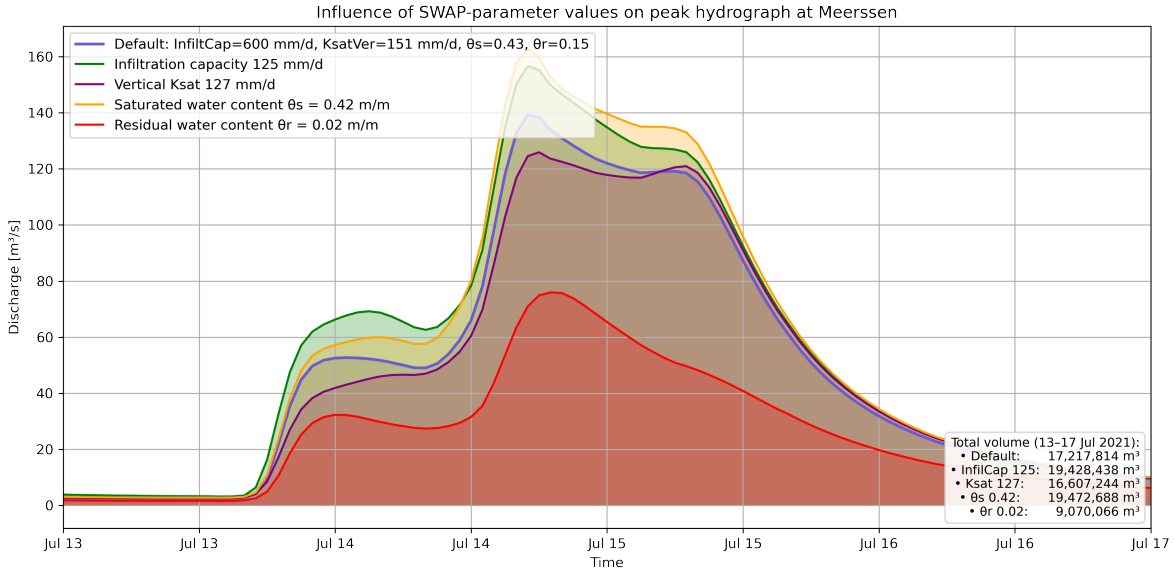

Figure 5.7: Simulated discharge at the catchment outlet (Meerssen) under default conditions and with individual SWAP-derived parameter values applied across the catchment. Each line represents the effect of adjusting a single parameter

spatial location of parameter changes strongly influences their effect on the flood hydrograph. Converting all agricultural fields in the 'Boven Geul' area to a rural NbS would therefore not mitigate flood peaks, but enhance the flood peak at the outlet. Given that the Boven Geul represents only about 28 km^2 (8% of the total catchment area), the net impact is limited.

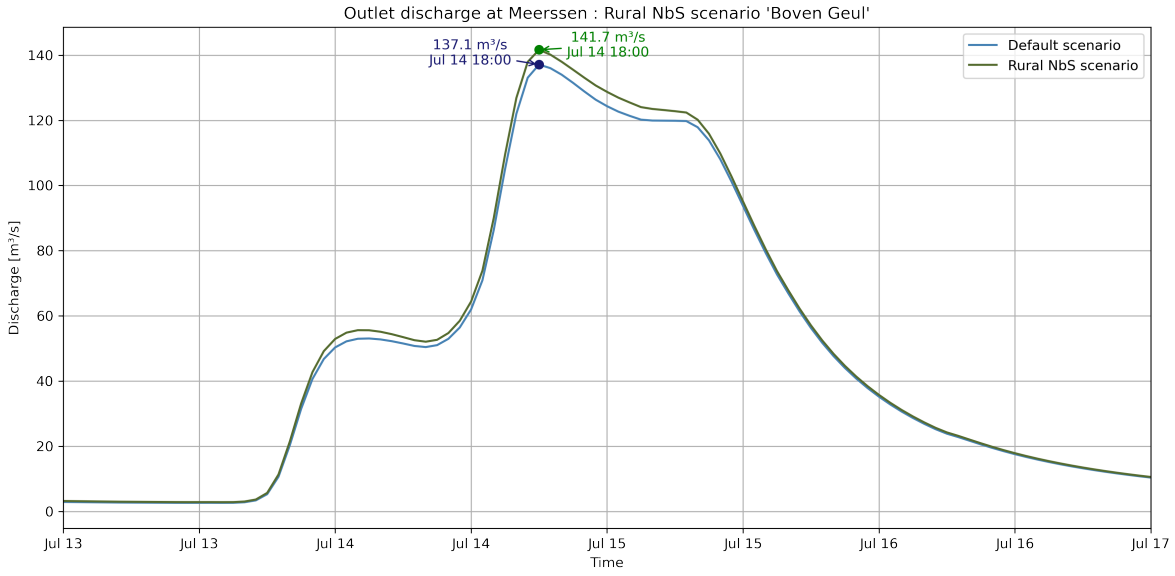

Figure 5.8: Simulated discharge when applying all the SWAP-values to mimic agroforestry for the 'Boven Geul' subcatchment

The second scenario applies the same parameter changes, but then applied in the Beneden Geul subcatchment. Here, the rural NbS produces the anticipated dampening effect on the flood hydrograph, although the impact remains very modest. The simulated peak flow is reduced by less than 2 m^3/s and occurs at approximately the same time as in the default scenario (Figure 5.9). The Beneden Geul covers about 50.5 km^2 (approximately 15% of the total catchment area), but because it is relatively urbanized, the potential for large-scale soil alterations is limited. Over the entire event, the total dis-

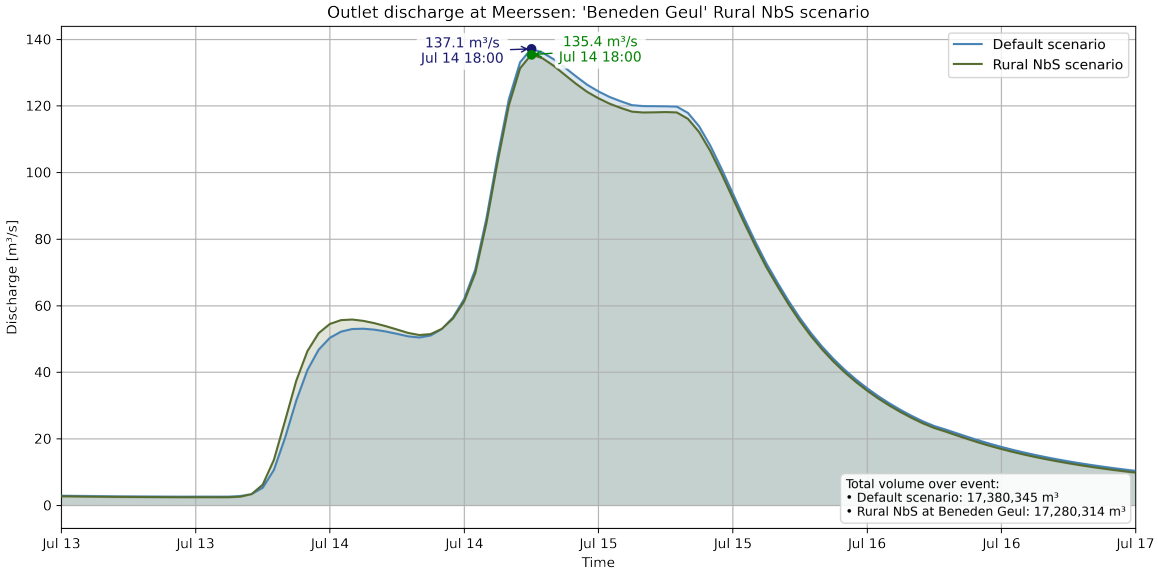

Figure 5.9: Simulated discharge when applying all the SWAP-values to mimic agroforestry for the 'Beneden Geul' subcatchment

charge volume is reduced by roughly 100,000 m^3.

5.2.3. Rural NbS-scenario applied catchment-wide

To assess the effect of large-scale implementation, SWAP-based parameters were applied to all permeable areas of the model, effectively converting them to sponge landscapes. Figure 5.10 shows that this scenario results in a pronounced decrease in the flood peak, but only a delay of two hours in timing. In addition, the total discharge volume leaving the catchment decreases by nearly 50%. These results suggest that, under a catchment-wide implementation scenario, creating sponge landscapes by implementing rural NbS can substantially reduce flood peak magnitude, but has only limited influence on peak timing in the Geul catchment.

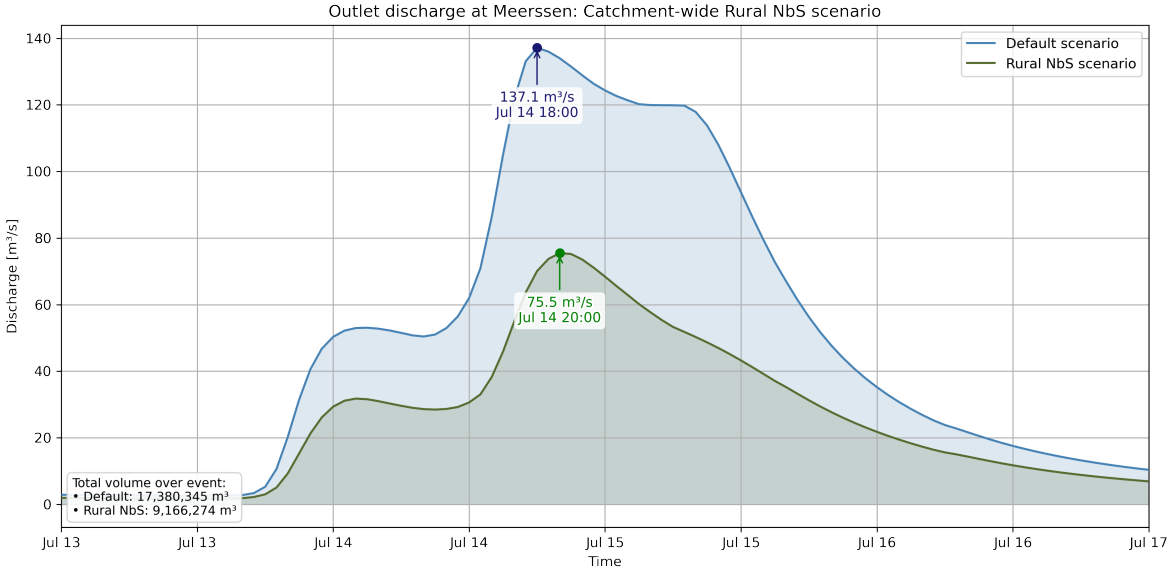

Figure 5.10: Simulated discharge when applying all the SWAP-values to mimic agroforesty for the whole catchment

6

Discussion

This chapter reflects on the findings of this study and places them in a broader hydrological and practical context. First, the most counterintuitive findings are discussed, followed by the limitations of the models and literature. Next, the potential implications of peak timing delay, as a result of large-scale rural NbS implementation, are explored for the confluence area. Finally, the practical feasibility and challenges of implementing such large-scale land-use changes are considered.

6.1. Discussion of the results

Overall, the results were consistent with my hypothesis. However, the rural NbS scenarios applied in subcatchments are a notable exception. In these cases, the differences relative to the default model were very small. For the Boven Geul, the simulated flood peak even increases rather than showing the expected attenuation. The explanation is probably methodological: the scenarios were simulated by lumping the modified parameters over the subcatchment, which removed much of the spatial heterogeneity that is particularly important in the Boven Geul (strong contrasts in soil types and hydrological connectivity). By smoothing the parameters, localized reductions in runoff generation are averaged out and their benefits could be muted. These findings motivate a more detailed assessment of the water storage capacity of the soil in this area. For the Beneden Geul, the limited effect likely reflects the high degree of urbanization and the relatively small distance to the outlet of the catchment.

6.2. Limitations modelling with SWAP

The SWAP model simulations used in this study represent a simplified approximation of the real-world water balance. An important limitation is that the simulations did not account for interflow as an explicit outward flux. This is a relevant process in the sloping terrain of the Geul catchment, where unsaturated lateral subsurface flow can occur. As a result, the simulated partitioning between infiltration, overland flow, and storage change may not fully reflect actual catchment behavior, and the model is likely to overestimate the storage change in the soil profile.

A second limitation is the absence of slope representation in the SWAP model setup. The simulations were conducted under flat-surface assumptions, which means no overland flow was used as model input. While this setup may represent the plateau areas of Zuid-Limburg, it does not capture the hydrological response of the many steep slopes present in the catchment. Consequently, the model results do not reflect processes such as slope-driven overland flow.

A third limitation concerns the meteorological forcing data used to drive the model. The simulations relied on precipitation and climate data from the Maastricht weather station, which recorded lower rainfall totals than were observed in the Geul catchment during the July 2021 flood event. This likely resulted in a conservative representation of soil-water dynamics and leading to an underestimation of the cumulative infiltration and overland flow.

6.3. Limitations used literature for the validation of the parameter mapping

Although the literature suggests a large increase in infiltration in rural NbS, comparing the results directly to the SWAP→wflow$_{sbm}$ mapping does not seem completely justified. The meta-analysis by Sun et al., 2018, used in part to validate the SWAP-based parameter values as a proxy for agroforestry, does not focus on extreme rainfall events. Although it synthesizes many datasets and distinguishes between initial and steady-state infiltration, much of the underlying evidence was collected under rainfall intensities and experimental conditions that differ markedly from those in this study. Therefore, values from the literature should be regarded primarily as qualitative ranges.

6.4. Limitations modelling with wflow SBM

In this section, the limitations of the model structure, parameters, and observation data are discussed. The items are numbered for clarity, but the order does not indicate prioritization.

1. **Model calibration:** The default wflow$_{sbm}$ model used in this study, was previously calibrated by Klein, 2022 for soil thickness and the KSHF parameter. However, further calibration is likely required, particularly because soil thickness strongly influences the simulated flood hydrographs.

2. **Observation quality:** The reliability of discharge observations during the July 2021 flood event is limited. In many subcatchments, complete records were unavailable, and the extreme flooding caused the river to overtop its 'banks', particularly near Valkenburg. As a result, the stage–discharge (Q–h) relationship downstream of Valkenburg is highly uncertain. This may explain the flat rising limb of observed hydrographs in the Meerssen subcatchment (Figure 5.2).

3. **Downstream discharge simulation:** The model has not been linked to a hydraulic model. As a result, backwater effects, floodplain inundation, and river routing peak propagation are not fully captured downstream, which may affect the timing and attenuation of simulated peak discharges. This contributes to the overestimating of the flood peak at Meerssen of the wflow$_{sbm}$ model.

4. **Groundwater storage representation:** The wflow_sbm model does not include a separate deep groundwater bucket. Deep groundwater flow is treated as leakage that permanently leaves the model domain, which may lead to an underestimation of baseflow contributions and a simplified representation of long-term storage changes.

5. **Model resolution:** The model used in this study had a grid size of 0.00833° (approximately 600 m × 925 m). While this resolution is adequate for general runoff simulation, a finer and locally calibrated model (subcatchment scale) might be necessary for assessing detailed land-use effects, as small-scale processes may be smoothed out at coarser resolutions.

6. **Choice of parameters for the mapping:** In this study, only parameters related to the "primary sponge function" of the soil were adjusted. However, real-world implementation of rural NbS would also influence parameters linked to 'secondary sponge function', such as Manning's roughness coefficient of the surface (N). Tree litter may increase surface roughness, so theoretically afforestation, agroforestry, and hedgerows could all increase N.

7. **Evapotranspiration neglected** Planting additional trees represents a significant hydrological intervention, as trees influence processes such as evaporation and transpiration. So if the rural nature-based solution includes trees, the measure will affect the model forcing input. This was not taken into account in the model simulations. However, under extreme rainfall conditions, the contribution of evaporation to the overall water balance is relatively small, and therefore its effect on simulated flood peaks is expected to be limited.

6.5. Broader system-scale effect of flood peak delay

Assessing the potential synchronization of flood peaks between the upstream catchment and its receiving basin is essential for determining whether rural NbS achieve effective flood mitigation or instead lead to an unintended amplification of flood risk at their confluence. This research gap was addressed

by comparing the timing of the simulated flood peak of the catchment-wide Rural NbS scenario to the timing of observed water levels in Meerssen and Borgharen during the flood event, as reported by (Strijker et al., 2023). The timing of the measured flood heights (Figure 6.1) shows that, assuming the simulated peak timing is realistic, the simulated two-hour delay remains within the five-hour timing window observed (Figure 6.1). Although the model predicts the flood peak somewhat earlier than the observatons, the results suggest that the two hour delay introduced by the Rural NbS scenario would not critically shift the coincidence of peak flows at the Geul–Meuse confluence.

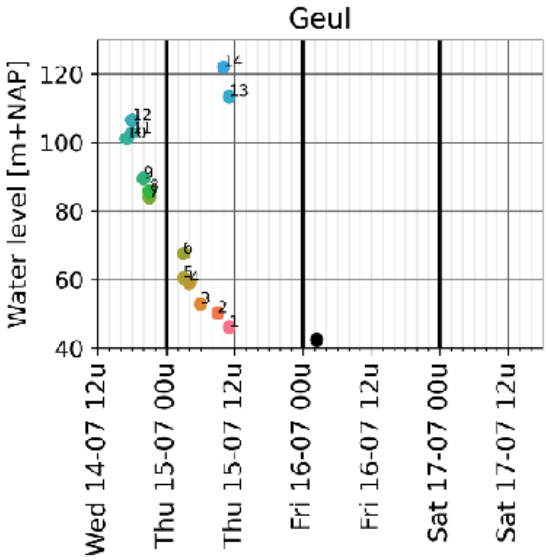

Figure 6.1: Timing and height of the peak water levels along the Geul. The pink dot (number 1) represents the location of the catchment outlet of the wflow_sbm model. The black dot indicates the moment and height of the water level at the measuring station in Meuse (Borgharen) close to the confluence (Strijker et al., 2023)

6.6. Practical perspective on catchment-wide scenario

From a practical standpoint, the catchment-wide scenario explored in this study should be viewed as a theoretical upper bound rather than a realistic policy strategy. Converting all unpaved agricultural land to sponge landscapes is unlikely to be feasible, as it would require extensive changes in land use and maybe farming practices throughout the catchment. Such a large-scale intervention would face social, economic and political challenges, including limited farmer willingness, potential reductions in agricultural productivity, the need for financial compensation, and significant policy support. In practice, the implementation of rural NbS would likely follow a more targeted approach, prioritizing the locations where measures are logistically and socially feasible over the locations with the highest potential hydrological impact.

7

Conclusion and Recommendations

7.1. Conclusion

This research aimed to evaluate how soil-water processes influence flood peak generation and mitigation in the Geul catchment under the extreme rainfall conditions of July 2021. By comparing process representation between SWAP and wflow$_{sbm}$, performing sensitivity analyses, and running rural NbS scenarios, several key conclusions were drawn. The following points directly address the research questions presented in Section 1.5:

1. **Differences between SWAP and wflow$_{sbm}$:** SWAP and wflow$_{sbm}$ are fundamentally different in their soil-water process representation. SWAP solves the Richards equation over the full soil profile, allowing direct specification of measured soil hydraulic properties. In contrast, wflow$_{sbm}$ uses mass-balance formulations and pedotransfer functions, resulting in parameter values that are less directly tied to measurable soil properties and often calibrated to match discharge observations.

2. **Soil-water parameter sensitivity in SWAP:** SWAP simulations revealed that infiltration and overland flow processes are most sensitive to the saturated water content (θ_{sat}) and the saturated hydraulic conductivity (K$_{sat}$). For a sandy soil column with a depth of 2 m, all rainfall from the July 2021 event could infiltrate, resulting in no overland flow generation.

3. **Soil-water parameter sensitivity in wflow$_{sbm}$:** The sensitivity analysis of wflow$_{sbm}$ showed that simulated flood hydrographs are most sensitive to KsatVer, θ_r, and θ_s. Adjusting θ_r and θ_s in the downstream subcatchments particularly could improve the model's ability to reproduce observed flood peaks, confirming that the soil's effective water storage capacity is a key control on downstream flood response.

4. **Representation of rural NbS in wflow$_{sbm}$:** SWAP-based sandy soil parameters were successfully transferred to wflow$_{sbm}$ to act as a proxy for multiple rural NbS. Scenario simulations demonstrated that the effect of these interventions is spatially dependent: downstream implementation had a different influence on river peak flow than upstream implementation, highlighting the importance of spatial targeting when designing rural NbS measures.

5. **Catchment-wide scenario impacts:** The catchment-wide rural NbS scenario produced a downstream flood peak reduction of approximately 50% and a two-hour delay in peak timing compared to the default model. Comparison with water level data from Strijker et al., 2023 showed that this delay still falls within the observed five-hour separation between the peaks of the Geul and the Meuse during the July 2021 event. This suggests that a catchment-wide implementation of 'improved soil' is unlikely to cause synchronization of peak flows at the Geul–Meuse confluence under similar extreme rainfall events.

In conclusion, this research demonstrated that soil-water processes in a distributed hydrological model have a significant influence on the simulated river peak flows. The results confirmed that the soil's

water storage capacity plays a key role in flood peak mitigation within the Geul catchment. Furthermore, well-located small rural NbS, can contribute to reducing peak discharges without increasing flood risk at the confluence. However, the reduction in peak flow achieved by these measures is relatively small, suggesting that they should be implemented in combination with traditional grey flood mitigation measures to achieve a truly flood-resilient catchment.

7.1.1. Recommendations for future work

Although this study provides valuable information on the role of soil-water processes and rural NbS in simulated river peak flows, several opportunities remain for further research:

- **Model refinement:** Conduct a more extensive calibration of wflow$_{sbm}$, particularly for the soil thickness. The soil depth may be the most important for saturation excess overland flow (Rogger et al., 2017; Rawlins et al., 1997). Next to this, consider coupling the wflow$_{sbm}$ model with a hydraulic model to better represent floodplain inundations and attenuation of the peak flow when propagating downstream (Paiva and Lima, 2024).
- **Higher spatial resolution:** Test the impact of using a finer grid resolution to capture small-scale rural NbS effects and heterogeneity in soil properties that may be smoothed out at coarser resolutions.
- **Dynamic vegetation representation:** Include parameter changes in the land use-land cover(LULC) map, such as the leaf area index (LAI), the rooting depth, and Manning's roughness coefficient to better represent the full hydrological effects of rural nature-based solutions in a modelling framework.
- **Improve soil data:** Future research should focus on measuring actual hydraulic conductivity and water retention curves for soils in the catchment, rather than relying on the default soil grid and the SWAP data. Using catchment-specific measurements, especially for the Boven Geul area in the Netherlands, would improve the reliability of simulated flood hydrographs.
- **Use projected forcing:** Evaluate the methodology with projected forcing rather than relying on a single event. This will test NbS performance across a wider range of different climatic and hydrological conditions and reduce event-specific biases.
- **Application other upstream catchments:** Future research could apply this methodology to energy-limited catchments, where evapotranspiration plays a more dominant role in the water balance. This would help to assess whether the findings regarding soil-water parameter sensitivity hold under different climatic and hydrological conditions. In addition, machine learning parameter calibration approaches could be explored to caibrate parameter sets more efficiently (Kapoor et al., 2023), which would facilitate the transferability of this modelling setup to other catchments.
- **Stakeholder analysis:** Combine hydrological modelling results with stakeholder analysis to evaluate farmer and other landowners willingness, and policy incentives to pinpoint potential areas to really implement large-scale rural nature-based solutions.

Bibliography

Alaoui, A., Lipiec, J., & Gerke, H. H. (2011). A review of the changes in the soil pore system due to soil deformation: A hydrodynamic perspective. *Soil and Tillage Research*, *115-116*, 1–15. https://doi.org/10.1016/J.STILL.2011.06.002

Alila, Y., Kuraś, P. K., Schnorbus, M., & Hudson, R. (2009). Forests and floods: A new paradigm sheds light on age-old controversies. *Water Resources Research*, *45*(8). https://doi.org/10.1029/2008WR007207

Allaban, A. (2025). *Regenbuffers in Limburg Hydrologische analyse over löss in Limburg* (tech. rep.). CTB3000-16: Bsc Eindwerk ; TU Delft.

Andréassian, V. (2004). Waters and forests: From historical controversy to scientific debate. *Journal of Hydrology*, *291*(1-2), 1–27. https://doi.org/10.1016/J.JHYDROL.2003.12.015

Ashagrie, A. G., De Laat, P. J., De Wit, M. J., Tu, M., & Uhlenbrook, S. (2006). Detecting the influence of land use changes on discharges and floods in the Meuse River Basin – the predictive power of a ninety-year rainfall-runoff relation? *Hydrology and Earth System Sciences*, *10*(5), 691–701. https://doi.org/10.5194/HESS-10-691-2006

Baptist, M. J., Penning, W. E., Duel, H., Smits, A. J., Geerling, G. W., van der Lee, G. E., & van Alphen, J. S. (2004). Assessment of the effects of cyclic floodplain rejuvenation on flood levels and biodiversity along the Rhine River. *River Research and Applications*, *20*(3), 285–297. https://doi.org/10.1002/RRA.778

Basche, A. D., & DeLonge, M. S. (2019). Comparing infiltration rates in soils managed with conventional and alternative farming methods: A meta-analysis. *Plos | One*, *14*(9). https://doi.org/10.1371/journal.pone.0215702

Bernsteinová, J., Bässler, C., Zimmermann, L., Langhammer, J., & Beudert, B. (2015). Changes in runoff in two neighbouring catchments in the Bohemian Forest related to climate and land cover changes. *Journal of Hydrology and Hydromechanics*, *63*(4), 342–352. https://doi.org/10.1515/JOHH-2015-0037

Bonfante, A., & Bouma, J. (2015). The role of soil series in quantitative land evaluation when expressing effects of climate change and crop breeding on future land use. *Geoderma*, *259-260*, 187–195. https://doi.org/10.1016/J.GEODERMA.2015.06.010

Bouaziz, L. J. E. (2021). Internal processes in hydrological models A glance at the Meuse basin from space. https://doi.org/10.4233/uuid:09d84cc1-27e2-4327-a8c7-207a75952061

Brown, A. E., Zhang, L., McMahon, T. A., Western, A. W., & Vertessy, R. A. (2005). A review of paired catchment studies for determining changes in water yield resulting from alterations in vegetation. *Journal of Hydrology*, *310*(1-4), 28–61. https://doi.org/10.1016/J.JHYDROL.2004.12.010

Bureau Stroming. (2022). *Analyse functioneren klimaatbuffers in het Geul stroomgebied tijdens extreme neerslag in juli 2021* (tech. rep.).

Calder, I. R., Reid, I., Nisbet, T. R., & Green, J. C. (2003). Impact of lowland forests in England on water resources: Application of the Hydrological Land Use Change (HYLUC) model. *Water Resources Research*, *39*(11). https://doi.org/10.1029/2003WR002042

Calder, I. R., Smyle, J., & Aylward, B. (2007). Debate over flood-proofing effects of planting forests [2]. *Nature*, *450*(7172), 945. https://doi.org/10.1038/450945B;KWRD

Çerçioğlu, M., Udawatta, R. P., & Anderson, S. H. (2025). Use of cover crops for sustainable management of soil condition and health: A review. https://doi.org/10.1016/j.soisec.2025.100177

Deltares. (2023). *Een watersysteemanalyse - wat leren we van het hoogwater van juli 2021?* (Tech. rep.).

de Moor, J. J., Kasse, C., van Balen, R., Vandenberghe, J., & Wallinga, J. (2008). Human and climate impact on catchment development during the Holocene - Geul River, the Netherlands. *Geomorphology*, *98*(3-4), 316–339. https://doi.org/10.1016/J.GEOMORPH.2006.12.033

de Moor, J. J., & Verstraeten, G. (2008). Alluvial and colluvial sediment storage in the Geul River catchment (The Netherlands) — Combining field and modelling data to construct a Late Holocene

sediment budget. *Geomorphology*, *95*(3-4), 487–503. https://doi.org/10.1016/J.GEOMORPH.2007.07.012

de Wit, M. (2008). *Van regen tot Maas* (M. Joenje & P. Bosschieter, Eds.; 1st). Uitgeverij Veen Magazines.

Eulderink, J. L. F. (2019). *Modelling and Assessing the Impacts of Large-Scale Hydropower Projects on the Ecohydrology of Rivers in Myanmar* (tech. rep.). http://repository.tudelft.nl/.

European Commission. (2014). *Natural Water Retention Measures Selecting, designing and implementing Capturing the multiple benefits of nature-based solutions Natural Water Retention Measures in Europe* (tech. rep.). http://nwrm.eu/measures-catalogue

European Commission. (2015). Towards an EU Research and Innovation policy agenda for Nature-Based Solutions & Re-Naturing Cities. https://doi.org/10.2777/765301

Gerrits, A. M., Savenije, H. H., Veling, E. J., & Pfister, L. (2009). Analytical derivation of the Budyko curve based on rainfall characteristics and a simple evaporation model. *Water Resources Research*, *45*(4). https://doi.org/10.1029/2008WR007308

Gourevitch, J. D., Singh, N. K., Minot, J., Raub, K. B., Rizzo, D. M., Wemple, B. C., & Ricketts, T. H. (2020). Spatial targeting of floodplain restoration to equitably mitigate flood risk. *Global Environmental Change*, *61*, 102050. https://doi.org/10.1016/J.GLOENVCHA.2020.102050

Gusev, E. M., Nasonova, O. N., & Dzhogan, L. Y. (2011). Modeling river runoff in Northwestern Russia with the use of land surface model SWAP and global databases. *Water Resources*, *38*(5), 571–582. https://doi.org/10.1134/S0097807811050101/METRICS

Heinen, M., Mulder, H. M., Bakker, G., Wösten, J. H., Brouwer, F., Teuling, K., & Walvoort, D. J. (2022). The Dutch soil physical units map: BOFEK. *Geoderma*, *427*. https://doi.org/10.1016/j.geoderma.2022.116123

Heinen, M., Mulder, M., van Dam, J., Bartholomeus, R., de Jong van Lier, Q., de Wit, J., de Wit, A., & Hack - ten Broeke, M. (2024). SWAP 50 years: Advances in modelling soil-water-atmosphere-plant interactions. *Agricultural Water Management*, *298*, 108883. https://doi.org/10.1016/J.AGWAT.2024.108883

Hersbach, H., Bell, B., Berrisford, P., Hirahara, S., Horányi, A., Muñoz-Sabater, J., Nicolas, J., Peubey, C., Radu, R., Schepers, D., Simmons, A., Soci, C., Abdalla, S., Abellan, X., Balsamo, G., Bechtold, P., Biavati, G., Bidlot, J., Bonavita, M., … Thépaut, J. N. (2020). The ERA5 global reanalysis. *Quarterly Journal of the Royal Meteorological Society*, *146*(730), 1999–2049. https://doi.org/10.1002/qj.3803

Ilstedt, U., Bargués Tobella, A., Bazié, H. R., Bayala, J., Verbeeten, E., Nyberg, G., Sanou, J., Benegas, L., Murdiyarso, D., Laudon, H., Sheil, D., & Malmer, A. (2016). Intermediate tree cover can maximize groundwater recharge in the seasonally dry tropics OPEN. https://doi.org/10.1038/srep21930

(IPCC), I. P. o. C. C. (2023). Weather and Climate Extreme Events in a Changing Climate. *Climate Change 2021 – The Physical Science Basis*, 1513–1766. https://doi.org/10.1017/9781009157896.013

IUCN. (2022). Nature-based Solutions in the Post-2020 Global Biodiversity Framework Targets. *IUCN Policy Brief*. https://www.carbontrust.com/resources/briefing-what-are-scope-3-

Jiang, J., Feng, S., Ma, J., Huo, Z., & Zhang, C. (2016). Irrigation management for spring maize grown on saline soil based on SWAP model. *Field Crops Research*, *196*, 85–97. https://doi.org/10.1016/J.FCR.2016.06.011

Kapoor, A., Pathiraja, S., Marshall, L., & Chandra, R. (2023). DeepGR4J: A deep learning hybridization approach for conceptual rainfall-runoff modelling. *Environmental Modelling and Software*, *169*. https://doi.org/10.1016/j.envsoft.2023.105831

Klein, A. C. (2022). *Hydrological Response of the Geul Catchment to the Rainfall in July 2021* (tech. rep.). Delft University of Technology. MSc Thesis. http://repository.tudelft.nl/.

Kroes, J., van Dam, J., Bartholomeus, R., Groenendijk, P., Heinen, M., Hendriks, R., Mulder, H., Supit, I., & van Walsum, P. (2017). *SWAP version 4* (tech. rep.). https://doi.org/10.18174/416321

Kumar, P., Debele, S. E., Sahani, J., Rawat, N., Marti-Cardona, B., Alfieri, S. M., Basu, B., Basu, A. S., Bowyer, P., Charizopoulos, N., Gallotti, G., Jaakko, J., Leo, L. S., Loupis, M., Menenti, M., Mickovski, S. B., Mun, S. J., Gonzalez-Ollauri, A., Pfeiffer, J., … Zieher, T. (2021). Nature-based solutions efficiency evaluation against natural hazards: Modelling methods, advantages

and limitations. *Science of The Total Environment*, *784*, 147058. https://doi.org/10.1016/J.SCITOTENV.2021.147058

Kwadijk, J., Slager, K., Bouaziz, L., & Becker, A. (2022). *Rapid assessment study on the Geul river basin Appendices with background material With contributions from: Acknowledgements* (tech. rep.). APPENDICES.

Laverde-Barajas, M., Corzo Perez, G. A., Chishtie, F., Poortinga, A., Uijlenhoet, R., & Solomatine, D. P. (2020). Decomposing satellite-based rainfall errors in flood estimation: Hydrological responses using a spatiotemporal object-based verification method. *Journal of Hydrology*, *591*, 125554. https://doi.org/10.1016/J.JHYDROL.2020.125554

Li, P., & Ren, L. (2019). Evaluating the effects of limited irrigation on crop water productivity and reducing deep groundwater exploitation in the North China Plain using an agro-hydrological model: II. Scenario simulation and analysis. *Journal of Hydrology*, *574*, 715–732. https://doi.org/10.1016/j.jhydrol.2019.03.034

Ministerie Infrastructuur en Waterstaat. (2022). Kamerbrief over rol Water en Bodem bij ruimtelijke ordening.

Mualem, Y. (1976). A new model for predicting the hydraulic conductivity of unsaturated porous media. *Water Resources Research*, *12*(3), 513–522. https://doi.org/10.1029/WR012i003p00513

Muishout, C. (2023). *The Hydrological Effect of Urban Nature-based Solutions on Catchment Scale A Case Study in the Geul Catchment* (tech. rep.). MSc Thesis. http://repository.tudelft.nl/.

Muys, B., Ellison, D., & Wunder, S. (2021). Key Questions on Forests in the EU, Q7: What role do forests play in the water cycle? *EFI*. https://doi.org/10.36333/k2a04

Overhoff, J., & Slager, K. (2024). *Evaluating nature-based solutions for flooding in the Geul catchment using openLISEM* (tech. rep.). MSc Thesis.

Paiva, R. C., & Lima, S. G. (2024). A Simple Model of Flood Peak Attenuation. *Water Resources Research*, *60*(2). https://doi.org/10.1029/2023WR034692

Peel, M. C., Finlayson, B. L., & Mcmahon, T. A. (2007). *Hydrology and Earth System Sciences Updated world map of the Köppen-Geiger climate classification* (tech. rep.). www.hydrol-earth-syst-sci.net/11/1633/2007/

Penning, E., Burgos, R. P., Mens, M., Dahm, R., & Bruijn, K. d. (2023). Nature-based solutions for floods AND droughts AND biodiversity: Do we have sufficient proof of their functioning? *Cambridge Prisms: Water*, *1*, e11. https://doi.org/10.1017/WAT.2023.12

Penning, E., Klein, A., Asselman, N., De Louw, P., Kaandorp, V., Van Geest, G., Kingma, V., & Schoonderwoerd, E. (2024). *Sponswerking van Landschappen in Nederland* (tech. rep.).

Rawlins, B. G., Baird, A. J., Trudgill, S. T., & Hornung, M. (1997). ABSENCE OF PREFERENTIAL FLOW IN THE PERCOLATING WATERS OF A CONIFEROUS FOREST SOIL. *Hydrological Processes*, *11*, 575–585. https://doi.org/10.1002/(SICI)1099-1085(199705)11:6

Richards, L. A. (1931). Capillary conduction of liquids through porous mediums. *Journal of Applied Physics*, *1*(5), 318–333. https://doi.org/10.1063/1.1745010

Rogger, M., Agnoletti, M., Alaoui, A., Bathurst, J. C., Bodner, G., Borga, M., Chaplot, V., Gallart, F., Glatzel, G., Hall, J., Holden, J., Holko, L., Horn, R., Kiss, A., Kohnová, S., Leitinger, G., Lennartz, B., Parajka, J., Perdigão, R., … Blöschl, G. (2017). Land use change impacts on floods at the catchment scale: Challenges and opportunities for future research. *Water Resources Research*, *53*(7), 5209–5219. https://doi.org/10.1002/2017WR020723

Rongen, G., Morales-Nápoles, O., & Kok, M. (2023). Using structured expert judgment to Estimate extreme river discharges: a case study of the Meuse River. https://doi.org/10.5194/egusphere-2023-39

Ruangpan, L., Vojinovic, Z., Di Sabatino, S., Leo, L. S., Capobianco, V., Oen, A. M., Mcclain, M. E., & Lopez-Gunn, E. (2020). Nature-based solutions for hydro-meteorological risk reduction: a state-of-the-art review of the research area. *Natural Hazards and Earth System Sciences*, *20*(1), 243–270. https://doi.org/10.5194/NHESS-20-243-2020

Rura Arnhem. (2018). *Actualisatie beschrijving laterale toestroming Maas* (tech. rep.). Rura Arnhem.

Saghafian, B., Farazjoo, H., Bozorgy, B., & Yazdandoost, F. (2008). Flood intensification due to changes in land use. *Water Resources Management*, *22*(8), 1051–1067. https://doi.org/10.1007/S11269-007-9210-Z/METRICS

Schellekens, J. (2011). *wFlow , a flexible hydrological model* (tech. rep.).

Seizarwati, W., & Syahidah, M. (2021). Rainfall-Runoff Simulation for Water Availability Estimation in Small Island Using Distributed Hydrological Model wflow. *IOP Conference Series: Earth and Environmental Science*, *930*(1), 012050. https://doi.org/10.1088/1755-1315/930/1/012050

Slager, K., Becker, A., Bouaziz, L., & Kwadijk, J. (2022). *Rapid assessment study on the Geul river basin: Screening of flood reduction measures* (tech. rep.).

Strijker, B., Asselman, N., De Jong, J., & Barneveld, H. (2023). The 2021 floods in the Netherlands from a river engineering perspective. *Journal of Coastal and Riverine Flood Risk*, *2*. https://doi.org/10.59490/jcrfr.2023.0006

Sun, D., Yang, H., Guan, D., Yang, M., Wu, J., Yuan, F., Jin, C., Wang, A., & Zhang, Y. (2018). The effects of land use change on soil infiltration capacity in China: A meta-analysis. *Science of The Total Environment*, *626*, 1394–1401. https://doi.org/10.1016/J.SCITOTENV.2018.01.104

Van de Westeringh, W. (1980). Soils and their geology in the Geul Valley. *Landbouwhogeschool Wageningen*. https://edepot.wur.nl/467976

Van Verseveld, W. J., Weerts, A. H., Visser, M., Buitink, J., Imhoff, R. O., Boisgontier, H., Bouaziz, L., Eilander, D., Hegnauer, M., Ten Velden, C., & Russell, B. (2022). Wflow_sbm v0.6.1, a spatially distributed hydrologic model: from global data to local applications. https://doi.org/10.5194/gmd-2022-182

Van Verseveld, W. J., Weerts, A. H., Visser, M., Buitink, J., Imhoff, R. O., Boisgontier, H., Bouaziz, L., Eilander, D., Hegnauer, M., Ten Velden, C., & Russell, B. (2024). Wflow-sbm v0.7.3, a spatially distributed hydrological model: From global data to local applications. *Geoscientific Model Development*, *17*(8), 3199–3234. https://doi.org/10.5194/GMD-17-3199-2024,

van Genuchten, M. T. (1980). A Closed form Equation for Predicting the Hydraulic Conductivity of Unsaturated Soils. *Soil Science Society of America Journal*, *44*(5), 892–898. https://doi.org/10.2136/SSSAJ1980.03615995004400050002X

van Winden, A., Otterman, E., Braakhekke, W., & van Deursen, W. (2014). *VASTHOUDEN in de BERGEN om AFVOEREN te vertragen* (tech. rep.).

Vertessy, R. A., & Elsenbeer, H. (1999). Distributed modeling of storm flow generation in an Amazonian rain forest catchment: Effects of model parameterization. *Water Resources Research*, *35*(7), 2173–2187. https://doi.org/10.1029/1999WR900051

Wang, L., Zhong, C., Gao, P., Xi, W., & Zhang, S. (2015). Soil infiltration characteristics in agroforestry systems and their relationships with the temporal distribution of rainfall on the loess plateau in China. *PLoS ONE*, *10*(4). https://doi.org/10.1371/journal.pone.0124767

Yang, Y., Yang, L., Villarini, G., Zhao, F., Huang, D., Vecchi, G. A., Wang, Q., Sun, Y., & Tian, F. (2025). Synchronization of global peak river discharge since the 1980s. *Nature Climate Change 2025 15:10*, *15*(10), 1084–1090. https://doi.org/10.1038/S41558-025-02427-6

Zeiger, S. J., & Hubbart, J. A. (2018). Quantifying land use influences on event-based flow frequency, timing, magnitude, and rate of change in an urbanizing watershed of the central USA. *Environmental Earth Sciences*, *77*(3), 1–15. https://doi.org/10.1007/S12665-018-7312-Y/FIGURES/6

A

Study Area

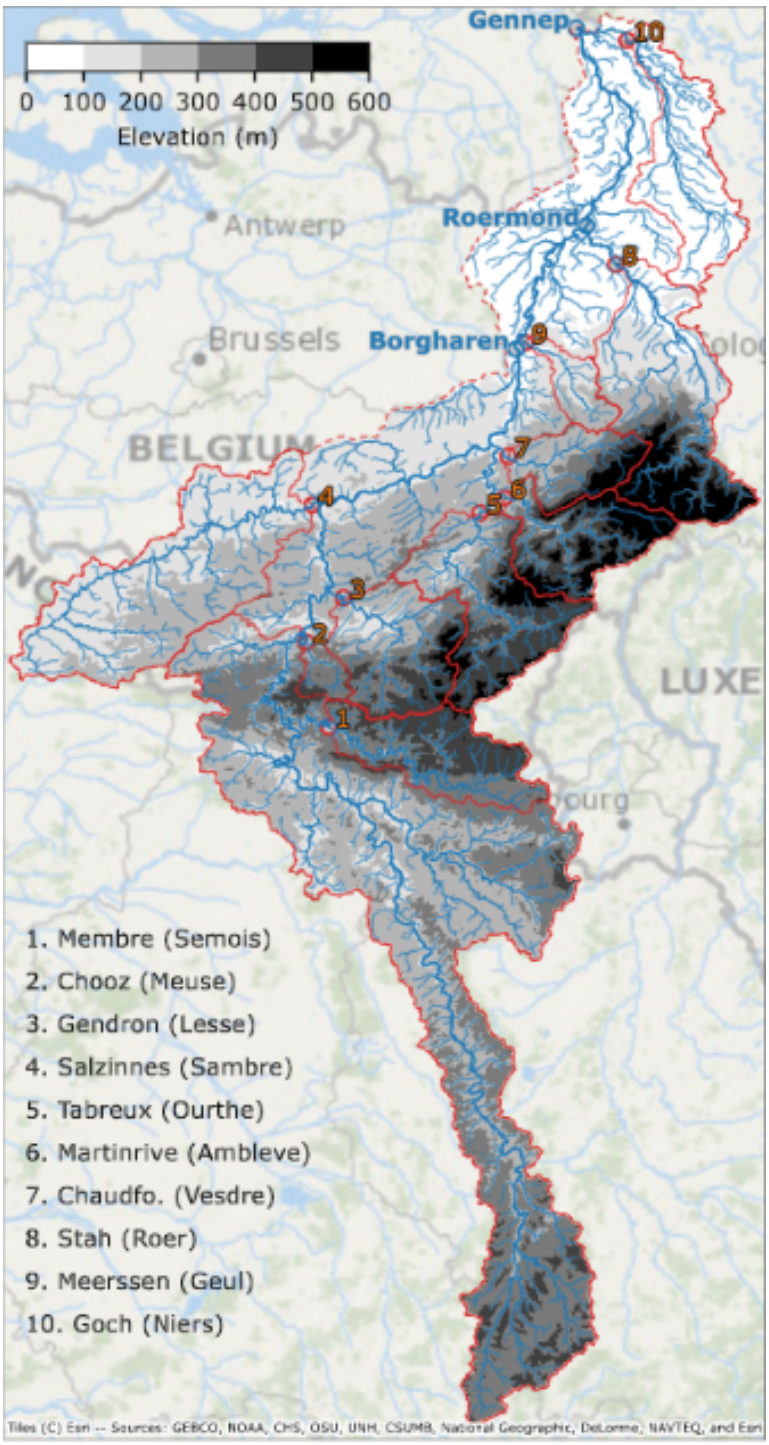

Figure A.1: Map of the Meuse basin with its upstream /tributary (Rongen et al., 2023)

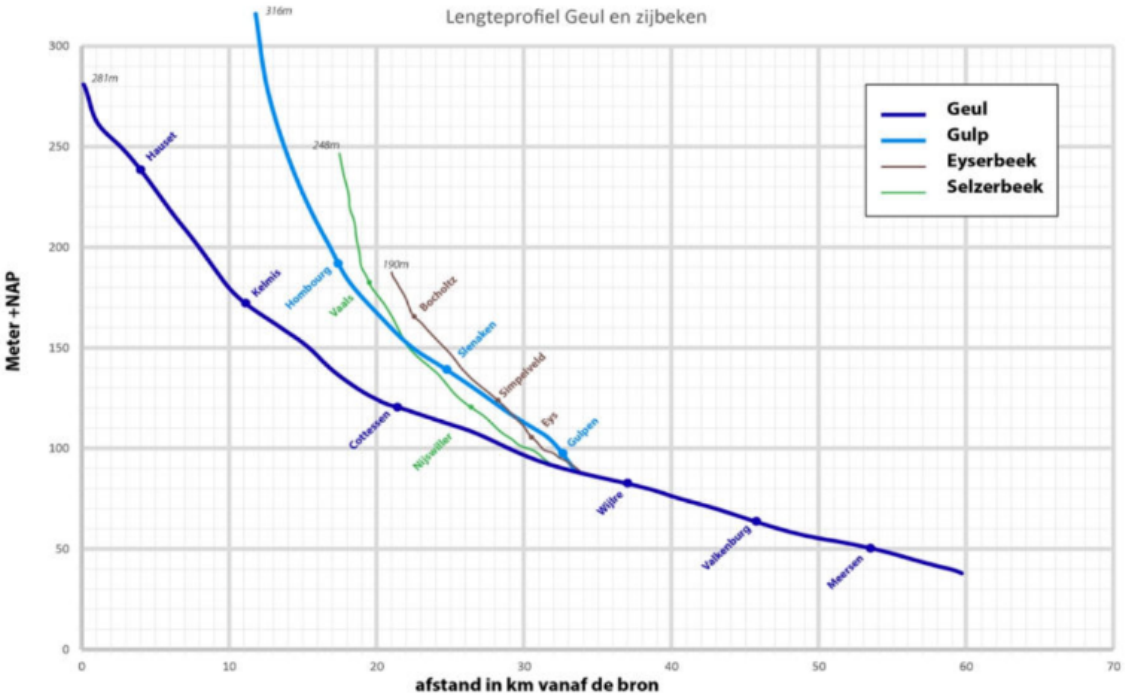

Figure A.2: Length and height profile of the Geul and its main tributaries: Gulp, Eyserbeek and Selzerbeek (van Winden et al., 2014).

B

Method

Main input file (*.swp)

- *General section*
  - Environment
  - Timing of simulation period
  - Timing of boundary conditions
  - Processes which should be simulated
  - Optional output files
- *Meteorology section*
  - Name of file with meteorological data
  - Rainfall intensity
- *Crop section*
  - Crop rotation scheme (calendar and files)
  - Crop data input file
  - Calculated irrigation input file
  - Crop emergence and harvest
  - Fixed irrigation parameters (Amount and quality of prescribed irrigation applications)
- *Soil water section*
  - Initial moisture condition
  - Ponding
  - Soil evaporation
  - Vertical discretization of soil profile
  - Soil hydraulic functions
  - Hysteresis of soil water retention function
  - Maximum rooting depth
  - Similar media scaling of soil hydraulic functions
  - Preferential flow due to soil volumes with immobile water
  - Preferential flow due to macro pores
  - Snow and frost
  - Numerical solution of Richards' equation
- *Lateral drainage section*
  - (optional) name of file with drainage input data
  - (optional) name of file with runon input data
- *Bottom boundary section*
  - (optional) name of file with bottom boundary conditions
  - selection out of 8 options
- *Heat flow section*
  - calculation method
- *Solute transport section*
  - Specify whether simulation includes solute transport or not
  - Top boundary and initial condition
  - Diffusion, dispersion, and solute uptake by roots
  - Adsorption
  - Decomposition
  - Transfer between mobile and immobile water volumes (if present)
  - Solute residence in the saturated zone

File with daily meteorological data (*.yyy)

- Radiation, temperature, vapour pressure, wind speed, rainfall and/or reference evapotranspiration,
- rainfall intensities

File with Detailed crop growth (*.crp) #

- *Crop section*
  - Crop height
  - Crop development
  - Initial values
  - Green surface area
  - Assimilation
  - Assimilates conversion into biomass
  - Maintenance respiration
  - Dry matter partitioning
  - Death rates
  - Crop water use
  - Salt stress
  - Interception
  - Root growth and density distribution
- *Calculated Irrigation section*
  - General
  - Irrigation time criteria
  - Irrigation depth criteria

File with Simple crop growth (*.crp) #

- *Crop section*
  - Crop development
  - Light extinction
  - Leaf area index or soil cover fraction
  - crop factor or crop height
  - rooting depth
  - yield response
  - soil water extraction by plant roots
  - salt stress
  - interception
  - Root density distribution and root growth
- *Calculated Irrigation section*
  - General
  - Irrigation time criteria
  - Irrigation depth criteria

File with drainage data (*.dra) #

- *Basic drainage section*
  - Table of drainage flux - groundwater level
  - Drainage formula of Hooghoudt or Ernst
  - Drainage and infiltration resistances
- *Extended drainage section*
  - Drainage characteristics
  - Surface water level of primary and/or secondary system
  - Simulation of surface water level
- Weir characteristics

Figure B.1: Summary of input data for the used SWAP model (Kroes et al., 2017)

Symbol	Description	Unit	Wflow.jl name
S_{canopy}	Canopy storage	mm	`canopystorage`
S_{snow}	Snow storage	mm	`snow`
$S_{\text{snow,liquid}}$	Amount of liquid water in the snowpack	mm	`snowwater`
S_{glacier}	Glacier storage	mm	`glacierstore`
$S_{\text{unsat, }n}$	Amount of water in the unsaturated zone, for layer n	mm	`ustorelayerdepth`
S_{sat}	Amount of water in saturated store	mm	`satwaterdepth`
S_{res}	Storage of reservoir	m^3	`volume`
S_{lake}	Lake storage	m^3	`storage`
H_{lake}	Water level lake	m	`waterlevel`
P	Precipitation	$\text{mm}\,t^{-1}$	`precipitation`
I_{total}	Total interception	$\text{mm}\,t^{-1}$	`interception`
$P_{\text{throughfall}}$	Throughfall	$\text{mm}\,t^{-1}$	`throughfall`
$F_{\text{available}}$	Infiltration rate of available water	$\text{mm}\,t^{-1}$	`avail_forinfilt`
F_{excess}	Infiltration excess water rate	$\text{mm}\,t^{-1}$	`infiltexcess`
$F_{\text{excess, sat}}$	Rate of water that cannot infiltrate due to saturated soil	$\text{mm}\,t^{-1}$	`waterexcess`
F_{act}	Actual infiltration rate	$\text{mm}\,t^{-1}$	`actinfilt`
$R_{\text{exfilt, sat}}$	Water exfiltrating under saturation excess conditions	$\text{m}\,t^{-1}$	`exfiltwater`
$R_{\text{exfilt, unsat}}$	Water exfiltrating from unsaturated store because of change in water table	$\text{mm}\,t^{-1}$	`exfiltustore`
R_{river}	Runoff from river fraction	$\text{mm}\,t^{-1}$	`runoff_river`
$R_{\text{open water}}$	Runoff from open-water fraction (excluding rivers)	$\text{mm}\,t^{-1}$	`runoff_land`
$E_{\text{open water}}$	Evaporation from open waterbodies (excluding rivers)	$\text{mm}\,t^{-1}$	`ae_openw_l`
E_{river}	Evaporation from rivers	$\text{mm}\,t^{-1}$	`ae_openw_r`
$E_{\text{act, sat}}$	Soil evaporation from the saturated store	$\text{mm}\,t^{-1}$	`soilevapsat`
$E_{\text{act, soil}}$	Soil evaporation from the unsaturated store	$\text{mm}\,t^{-1}$	–
$E_{\text{trans, sat}}$	Transpiration from the saturated store	$\text{mm}\,t^{-1}$	`actevapsat`
$\sum_{n=1}^{m} E_{\text{trans, unsat, }n}$	Transpiration from the unsaturated store for m unsaturated soil layers	$\text{mm}\,t^{-1}$	`ae_ustore`
C_{act}	Actual capillary rise	$\text{mm}\,t^{-1}$	`actcapflux`
L	Leakage	$\text{mm}\,t^{-1}$	`actleakage`
R_{input}	Net recharge to the saturated store	$\text{mm}\,t^{-1}$	`recharge`
$Q_{\text{subsurface}}$	Subsurface flow	$\text{m}^3\,\text{d}^{-1}$	`ssf`
$Q_{\text{transfer, act, }m}$	Transfer of water from unsaturated soil layer m to saturated store	$\text{mm}\,t^{-1}$	`transfer`
Q	Surface flow in the kinematic wave	$\text{m}^3\,\text{s}^{-1}$	`q_av*`
$Q_{\text{in, lake}}$	Lake inflow	$\text{m}^3\,t^{-1}$	`inflow`
$Q_{\text{out, lake}}$	Lake outflow	$\text{m}^3\,t^{-1}$	`totaloutflow`
P_{lake}	Lake average precipitation	$\text{mm}\,t^{-1}$	`precipitation`
E_{lake}	Lake average evaporation	$\text{mm}\,t^{-1}$	`evaporation`
$Q_{\text{in, res}}$	Reservoir inflow	$\text{m}^3\,t^{-1}$	`inflow`
$Q_{\text{out, res}}$	Reservoir outflow	$\text{m}^3\,t^{-1}$	`totaloutflow`
P_{res}	Reservoir average precipitation	$\text{mm}\,t^{-1}$	`precipitation`
$E_{\text{pot, res}}$	Reservoir average evaporation	$\text{mm}\,t^{-1}$	`evaporation`

Figure B.2: Overview of the state variables and fluxes used in the wflow_sbm model. The table lists the symbol, description, unit, and corresponding variable name in the Wflow.jl implementation (Van Verseveld et al., 2024).

Symbol	Description	Unit	Wflow.jl name	Default value
P	Precipitation	$\mathrm{mm}\,t^{-1}$	`precipitation`	–
$E_{\mathrm{pot,\,total}}$	Potential evapotranspiration	$\mathrm{mm}\,t^{-1}$	`potential_evaporation`	–
T_{air}	Mean air temperature	°C	`temperature`	–
z_{soil}	Soil depth	mm	`soilthickness`	2000.0
θ_{s}	Saturated soil water content	$\mathrm{mm\,mm^{-1}}$	θ_{s}	0.6
θ_{r}	Residual soil water content	$\mathrm{mm\,mm^{-1}}$	θ_{r}	0.01
f_{paved}	Fraction of compacted soil (or paved)	–	`pathfrac`	0.01
$f_{\mathrm{open\ water}}$	Open-water fraction (excluding rivers)	–	`waterfrac`	0.0
f_{river}	River fraction	–	`riverfrac`	–
$c_{\mathrm{infiltration,\,unpaved}}$	Infiltration capacity of non-compacted soil	$\mathrm{mm}\,t^{-1}$	`infiltcapsoil`	$100.0\,\mathrm{mm\,d^{-1}}$
$c_{\mathrm{infiltration,\,paved}}$	Infiltration capacity of compacted soil	$\mathrm{mm}\,t^{-1}$	`infiltcappath`	$10.0\,\mathrm{mm\,d^{-1}}$
z_{rooting}	Rooting depth	mm	`rootingdepth`	750.0
$\frac{E_{\mathrm{sat}}}{P_{\mathrm{sat}}}$	Gash interception model parameter	–	`e_r`	0.1
LAI	Leaf area index	$\mathrm{m^2\,m^{-2}}$	`leaf_area_index`	–
S_{leaf}	Specific leaf storage	mm	`sl`	–
$S_{\mathrm{canopy,\,max}}$	Canopy storage capacity	mm	`cmax`	1.0
$f_{\mathrm{canopygap}}$	Canopy gap fraction	–	`canopygapfraction`	0.1
$S_{\mathrm{wood,\,max}}$	Storage capacity, woody parts of vegetation	mm	`swood`	–
k	Extinction coefficient	–	`kext`	–
c_{rd}	Model parameter controlling the sigmoid function, for the fraction of wet roots	$\mathrm{mm^{-1}}$	`rootdistpar`	−500.0
$z_{\mathrm{cap,\,maxdepth}}$	Critical water depth beyond which capillary rise ceases	mm	`cap_hmax`	2000.0
n_{cap}	Empirical coefficient controlling capillary rise	–	`cap_n`	2.0
K_{v0}	Vertical saturated hydraulic conductivity at the soil surface	$\mathrm{mm}\,t^{-1}$	kv_0	$3000.0\,\mathrm{mm\,d^{-1}}$
f_{Kv}	Scaling parameter for vertical saturated hydraulic conductivity	$\mathrm{mm^{-1}}$	`f`	0.001
c_n	Brooks–Corey power coefficient	–	`c`	10.0
h_b	Air entry value	cm	`hb`	10.0
L_{max}	Maximum allowed leakage	$\mathrm{mm}\,t^{-1}$	`maxleakage`	$0.0\,\mathrm{mm\,d^{-1}}$
f_{Kh0}	Multiplication factor applied to K_{v0} (for lateral subsurface flow)	–	–	1.0
$f_{\mathrm{Kv},\,n}$	Multiplication factor (correcting vertical saturated hydraulic conductivity)	–	`kvfrac`	1.0
s_{ddf}	Degree-day-melt factor snow	$\mathrm{mm}\,t^{-1}\,°\mathrm{C}^{-1}$	`cfmax`	$3.75653\,\mathrm{mm\,d^{-1}\,°C^{-1}}$
$s_{\mathrm{fall},\,T\ \mathrm{threshold}}$	Temperature threshold for snowfall	°C	`tt`	0.0
$s_{\mathrm{fall},\,T\ \mathrm{interval}}$	Temperature threshold interval for snowfall	°C	`tti`	1.0
$s_{\mathrm{melt},\,T\ \mathrm{threshold}}$	Temperature threshold for snowmelt	°C	`ttm`	0.0
s_{whc}	Water-holding capacity of snow	–	`whc`	0.1
$g_{\mathrm{melt},\,T\ \mathrm{threshold}}$	Temperature threshold for glacier melt	°C	`g_tt`	0.0
g_{ddf}	Degree-day-melt factor glacier	$\mathrm{mm}\,t^{-1}\,°\mathrm{C}^{-1}$	`g_cfmax`	$3.0\,\mathrm{mm\,d^{-1}\,°C^{-1}}$
f_{glacier}	Fraction covered by a glacier	–	`glacierfrac`	0.0
S_{glacier}	Glacier storage	mm	`glacierstore`	5500.0
$g_{\mathrm{snow\ to\ firn}}$	Fraction of snow that is converted into firn	t^{-1}	`g_sifrac`	$0.001\,\mathrm{d^{-1}}$
w_{soil}	Weighting coefficient for near-surface soil temperature	t^{-1}	`w_soil`	$0.1125\,\mathrm{d^{-1}}$
$f_{\mathrm{red,\,frozen}}$	Controlling infiltration reduction factor	–	`cf_soil`	0.038
$c_{\mathrm{land\ slope}}$	Slope of the land surface	$\mathrm{m\,m^{-1}}$	β_{l}	–
$c_{\mathrm{river\ slope}}$	Slope of river	$\mathrm{m\,m^{-1}}$	`sl`	–
A_{res}	Reservoir area	$\mathrm{m^2}$	`area`	–
$Q_{\mathrm{min\ req.}}$	Minimum flow requirement downstream of the reservoir	$\mathrm{m^3\,s^{-1}}$	`demandrelease`	–
$Q_{\mathrm{max,\,res}}$	Maximum release capacity spillway	$\mathrm{m^3\,s^{-1}}$	`maxrelease`	–
$S_{\mathrm{res,\,max}}$	Maximum storage of the reservoir	$\mathrm{m^3}$	`maxvolume`	–
$f_{\mathrm{res,\,min}}$	Target minimum storage fraction	–	`targetminfrac`	–
$f_{\mathrm{res,\,max}}$	Target maximum storage fraction	–	`targetmaxfrac`	–
A_{lake}	Lake area	$\mathrm{m^2}$	`area`	–
$H_{0,\,\mathrm{lake}}$	Water level lake threshold (below this threshold no outflow occurs)	m	`threshold`	–
H_{lake}	Water level lake	m	`waterlevel`	–
α_{lake}	Lake rating curve coefficient	$\mathrm{m\,s^{-1\,(a)}}$, $\mathrm{m^{\frac{3}{2}}\,s^{-1\,(b)}}$	`b`	–
β_{lake}	Lake rating curve exponent	–	`e`	–
n_{land}	Manning's roughness (overland flow)	$\mathrm{s\,m^{-\frac{1}{3}}}$	`n`	0.072
n_{river}	Manning's roughness (river flow)	$\mathrm{s\,m^{-1/3}}$	`n`	0.036
x_{river}	River length	m	`dl`	–
w_{river}	River width	m	`width`	–
h_{bankfull}	River bankfull depth	m	`bankfull_depth`	1.0

Figure B.3: Overview of the forcing variables and model parameters used in the wflow_sbm model. The table lists each variable or parameter along with its symbol, description, unit, Wflow.jl name, and default value where applicable. Forcing variables include meteorological inputs such as precipitation, potential evaporation, and temperature. Model parameters cover soil, vegetation, snow, reservoir, and river properties that control hydrological processes in the model (Van Verseveld et al., 2024).

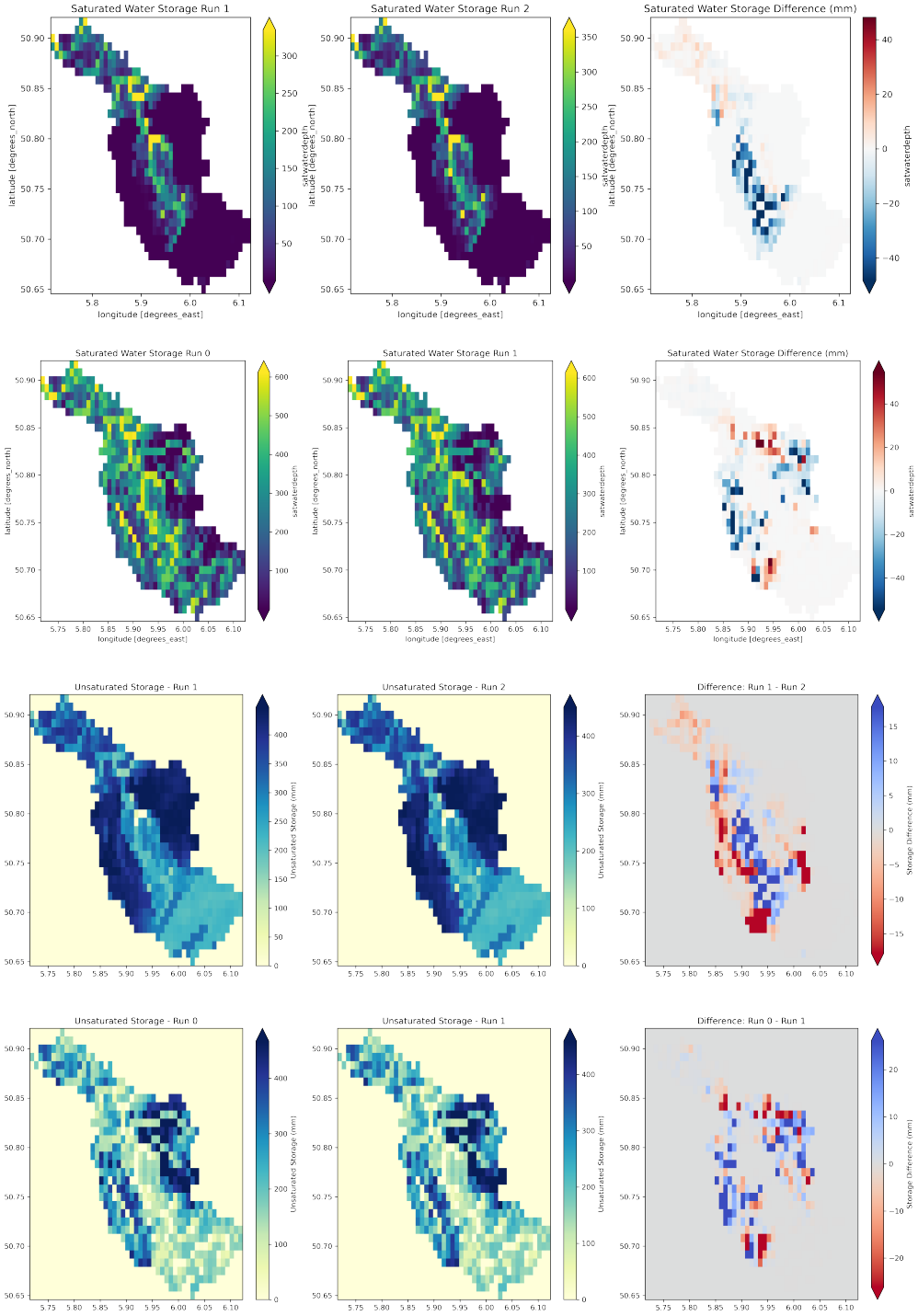

Figure B.4: Comparison of spin-up scenarios. Top: 6-hourly saturated state results. Second: Hourly saturated state results. Third: 6-hourly unsaturated state results. Bottom: Hourly unsaturated state results.

C

Comparison of proces approaches in SWAP and wflow$_{sbm}$

Hydrologic process	Approach in SWAP	Parameters in SWAP	Approach in wflow SBM	Parameters in wflow SBM
Interception	Analytical Gash model and Von Hoyningen-Hüne & Braden equation	LAI in coupled crop model	Analytical Gash model	LAI
Infiltration	Upperboundary Richard's equation	All VGM parameters	Controlled by (empirical) allocation and infiltration model parameters	InFiltCapSoil, InfiltCapPath, PathFrac
Vertical unsaturated flow	Richard's equation	All VGM parameters	Divided intro three mass buckets and transfer based on Brooks-Corey equation	KsatVer, θ_s, θ_r, f, c
Unsaturated lateral flow	Coupled drainage model	Drainage method	-	-
Groundwater recharge	Modified VGM equation with Ksat,exp	Ksat at bottom boundary	Controlled by leakage parameter and Brooks–Corey equation	MaxLeakage
Saturated lateral flow	Coupled drainage model	N in coupled drainage model	Gradient-based with vertical conductivity multiplication factor	KSHF
Overland flow	Only runoff generation (no routing)	-	Kinematic wave approach	N_{land}

Table C.1: Detailed comparison of hydrologic processes working on the soil cover and column as approached in the SWAP and wflow$_{sbm}$ modelling frameworks.

D

Sensitivity analysis in SWAP

				INITIALLY PRESENT	RESULTS				
				Soil water [cm]	Runoff [cm]	Infiltration [cm]	Exfiltration [cm]	Downward Seepage [cm	storage change [cm]
Scenarios									
Soil type	Changing parameter	x Ratio	Value						
Sand (B2/O2)	-	1,00	-	26,95	0,00	11,98	3,38	1,21	7,39
Sand	Ores	20,00	0,40	-	-	-	-	-	-
Sand	Ores	1,50		28,33	0,00	11,98	3,38	1,19	7,41
Sand	Ores	0,50		25,56	0,00	11,98	3,38	1,22	7,38
Sand	Osat	1,50		39,04	0,00	11,98	3,38	1,39	7,21
Sand	Osat	0,50		14,86	0,00	11,98	3,38	2,18	6,42
Sand	Osat	2,20	0,95	61,40	0,00	11,98	3,38	1,61	6,98
Sand	Ksat	1,50		26,95	0,00	11,98	3,38	1,56	7,04
Sand	Ksat	0,50		26,95	0,00	11,98	3,38	0,75	7,85
Sand	Ksat	0,25		26,95	1,21	10,77	3,38	0,45	6,94
Sand	Ksat	0,33		26,95	0,46	11,52	3,38	0,56	7,58
Sand	Alfa	1,50		20,92	0,00	11,98	3,38	0,38	8,22
Sand	Alfa	0,50		40,96	0,00	11,98	3,38	6,23	2,37
Sand	Npar	1,50		10,66	0,00	11,98	3,37	0,49	8,12
Sand	Npar	0,67	1,01	76,76	7,02	4,91	0,76	3,12	1,03
Sand	Lexp	1,50		26,95	0,00	11,98	3,38	1,14	7,46
Sand	Lexp	0,50		26,95	0,00	11,98	3,38	1,28	7,32
Sand	Lexp	24,00	-25,00	26,95	0,00	11,98	2,38	32,25	-22,65
Sand	Lexp	-24,00	25,00	26,95	0,23	11,78	1,93	0,00	9,85
Sand	Alfaw	1,50		26,95	0,00	11,98	3,38	1,21	7,39
Sand	Alfaw	0,50		26,95	0,00	11,98	3,38	1,21	7,39
Sand	Alfaw	36,00	1,00	26,95	0,00	11,98	3,38	1,21	7,39
Sand	Hentry	-40,00	-40,00	33,86	0,00	11,98	3,38	5,58	3,02
Clay (B11/O13)	-	1,00	-	99,68	3,61	8,35	3,36	0,18	4,81
Clay	Ores	40,00	0,40	110,28	4,89	7,06	3,35	1,11	2,60
Clay	Ores	1,50		99,77	3,64	8,31	3,36	0,18	4,77
Clay	Ores	0,50		99,64	3,62	8,34	3,36	0,18	4,80
Clay	Osat	1,50		150,35	3,03	8,93	3,36	0,19	5,38
Clay	Osat	0,50		50,75	4,28	7,67	3,35	0,17	4,15
Clay	Osat	1,60	0,95	164,71	2,93	9,03	3,36	0,19	5,48
Clay	Ksat	1,50		99,68	2,84	9,12	3,36	0,26	5,50
Clay	Ksat	0,50		99,68	5,80	6,15	3,35	0,10	2,70
Clay	Ksat	0,22	1,00	99,68	7,62	4,32	3,34	0,05	0,94
Clay	Ksat	221,00	1000,00	99,68	0,00	11,98	3,38	14,00	-5,40
Clay	Alfa	1,50		96,58	3,78	8,18	3,35	0,11	4,71
Clay	Alfa	0,50		104,55	3,12	8,84	3,36	0,41	5,07
Clay	Npar	1,50		48,21	0,00	26,39	2,69	-14,37	did not solve
Clay	Npar	3,60	4,00	3,90	0,00	11,99	0,60	14,68	did not solve
Clay	Lexp	1,50		99,68	3,41	8,55	3,36	0,24	4,95
Clay	Lexp	0,50		99,68	3,84	8,12	3,35	0,14	4,62
Clay	Lexp	4,20	-25,00	99,68	2,46	9,50	3,37	1,23	4,90
Clay	Lexp	-4,20	25,00	99,68	4,74	7,22	2,48	0,01	4,73
Clay	Alfaw	1,50		99,68	3,61	8,35	3,36	0,18	4,81
Clay	Alfaw	0,50		99,68	3,61	8,35	3,36	0,18	4,81
Clay	Alfaw	51,28	1,00	99,68	3,61	8,35	3,36	0,18	4,81
Clay	Hentry	-40,00	-40,00	104,60	0,00	11,98	3,38	12,73	-4,13
Silt (B14/O14)	-	1,00	-	67,67	5,60	6,35	3,35	7,09	-4,09
Silt	Ores	40,00	0,40	78,14	12,12	3,46	4,92	50,11	2,22
Silt	Ores	1,50		67,94	5,64	6,31	3,35	7,03	-4,08
Silt	Ores	0,50		67,54	5,58	6,37	3,35	7,12	-4,10
Silt	Osat	1,50		101,37	4,86	7,10	3,36	7,94	-4,21
Silt	Osat	0,50		33,97	6,58	5,37	3,35	5,65	-3,63
Silt	Osat	2,30	0,95	164,76	4,02	7,94	3,37	9,06	-4,48
Silt	Ksat	1,50		67,67	4,52	7,45	3,36	9,49	-5,41
Silt	Ksat	0,50		67,67	6,95	5,00	3,35	4,29	-2,63
Silt	Ksat	0,25		67,67	7,81	4,13	3,34	2,52	-1,73
Silt	Ksat	125	100,00	67,67	0,00	11,98	3,38	40,58	-31,98
Silt	Alfa	1,50		62,04	5,80	6,14	3,35	4,88	-2,08
Silt	Alfa	0,50		73,53	5,00	6,96	3,36	10,70	-7,10
Silt	Npar	1,50		63,68	1,26	10,72	3,38	14,47	-7,12
Silt	Npar	0,77	1,01	77,59	11,01	0,90	0,54	0,05	0,31
Silt	Lexp	1,50		67,67	5,60	6,35	3,35	7,21	-4,21
Silt	Lexp	0,50		67,67	5,60	6,35	3,35	6,97	-3,98
Silt	Lexp	12,50	-25,00	67,67	0,00	11,98	3,38	46,81	-38,21
Silt	Lexp	-12,50	25,00	67,67	7,10	4,85	2,55	1,06	1,24
Silt	Alfaw	1,50		67,67	5,60	6,35	3,35	7,09	-4,09
Silt	Alfaw	0,50		67,67	5,60	6,35	3,35	7,09	-4,09
Silt	Alfaw	196,00	1,00	67,67	5,60	6,35	3,35	7,09	-4,09
Silt	Hentry	-40,00	-40,00	68,66	1,74	10,23	3,37	11,42	-4,56

Figure D.1: Parameter sensitivity analysis for SWAP

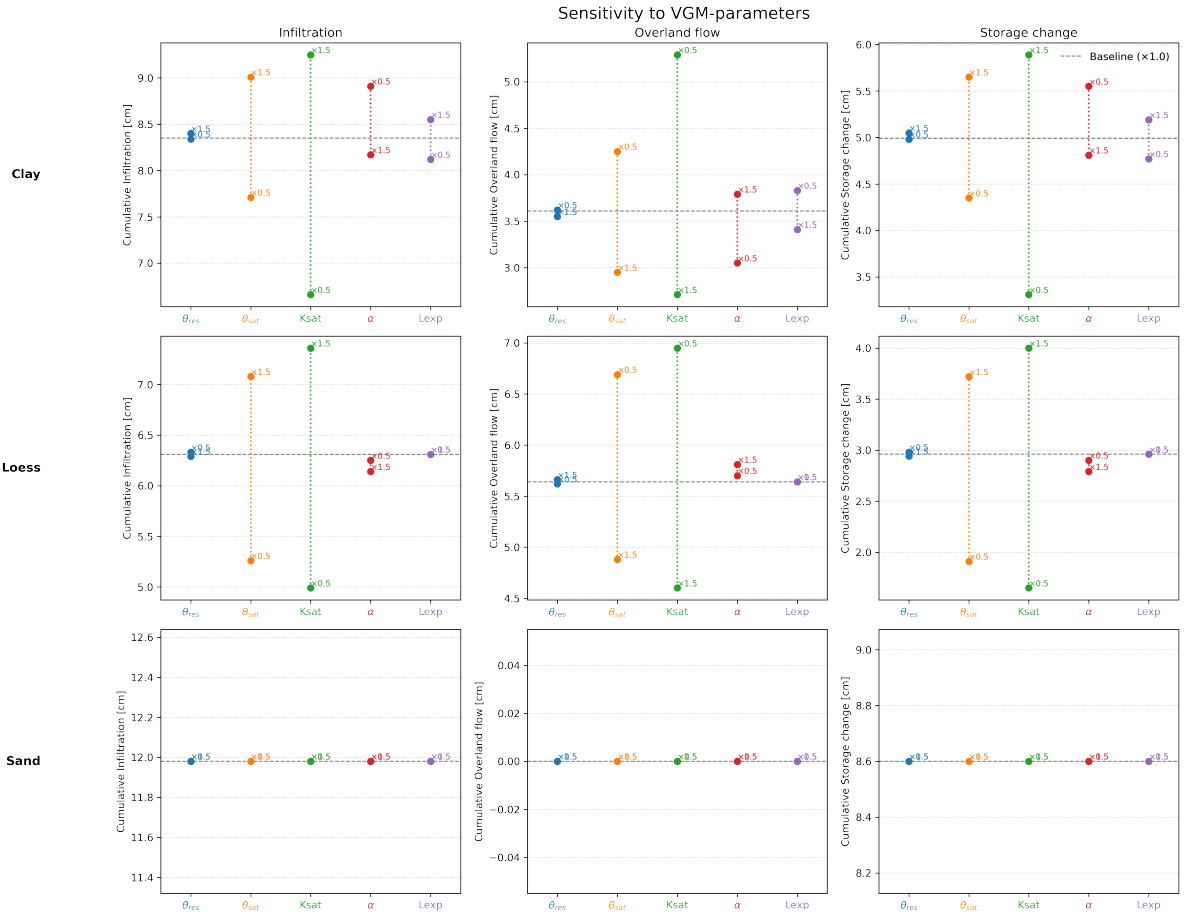

Figure D.2: Sensitivity analysis of Van Genuchten–Mualem soil hydraulic parameters on cumulative infiltration, overland flow, and storage change in the soil column, simulated with the SWAP model with an impermeable layer underneath (July 2021).

E

Sensitivity analysis in wflow$_{sbm}$

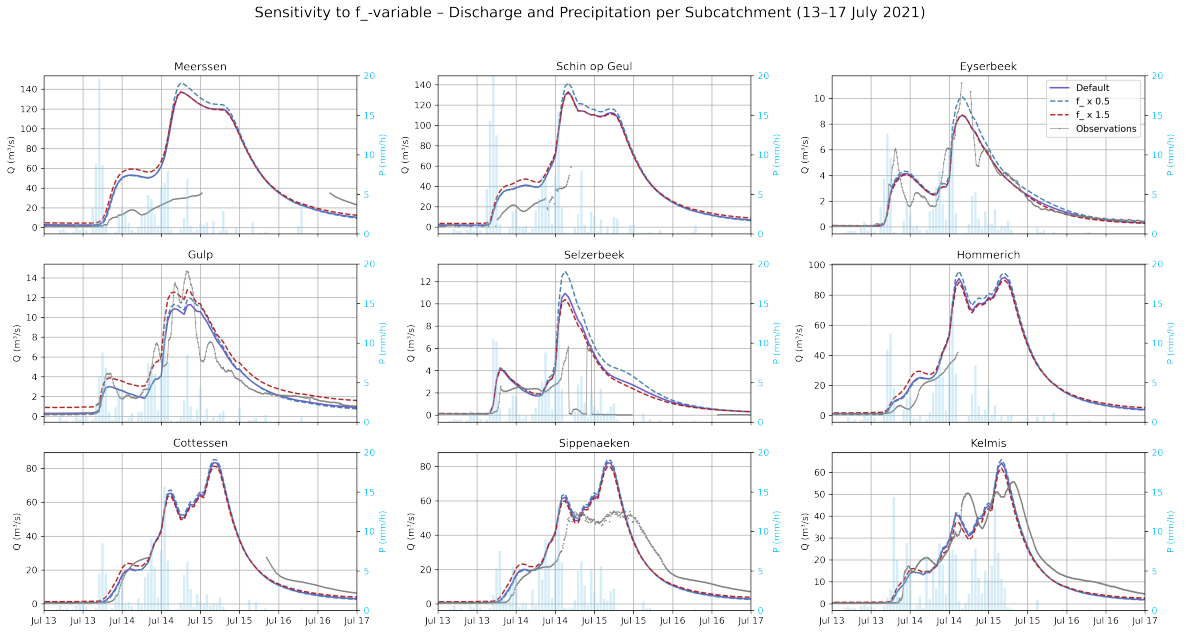

Figure E.1: Simulated flood hydrograph sensitivity to the f parameter for nine subcatchments during the July 2021 flood event. Shown are the default model (purple), scenarios with f × 0.5 (blue dashed), × 1.5 (red dashed), with precipitation forcing (bars, right axis) and observed discharge (grey) where available.

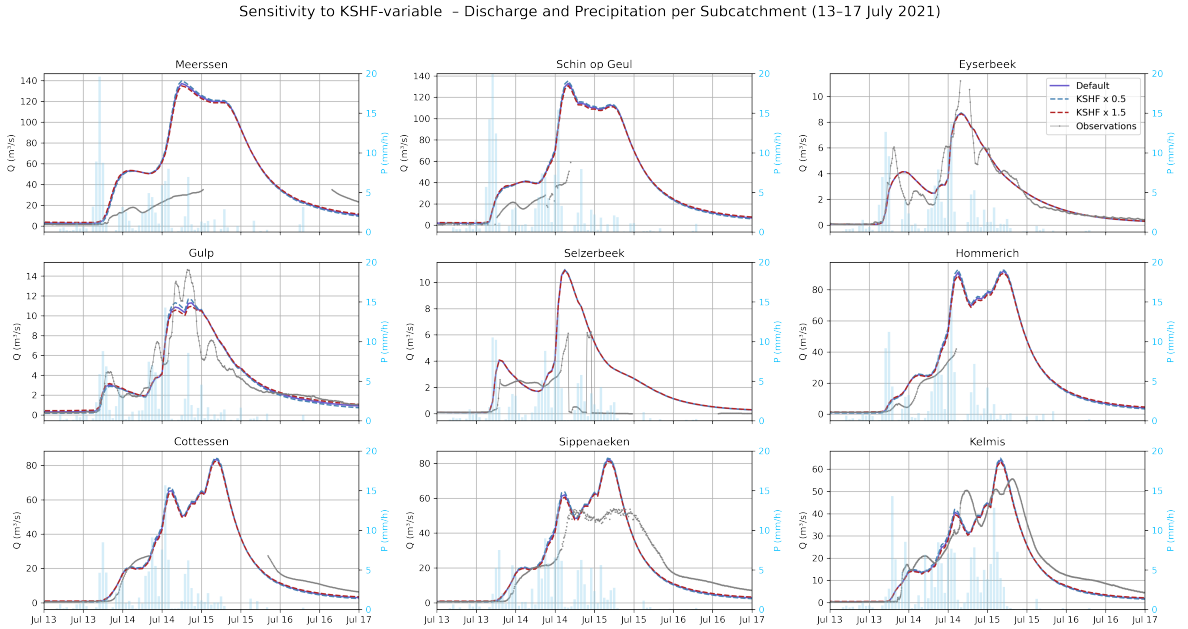

Figure E.2: Simulated flood hydrograph sensitivity to KSatHorFrac (KSHF) for nine subcatchments during the July 2021 flood event. Shown are the default model (purple), scenarios with KSHF × 0.5 (blue dashed), × 1.5 (red dashed), with precipitation forcing (bars, right axis) and observed discharge (grey) where available